Climate Repair - Ice Thickening

Jacob Pantling

Final Report

Technical Abstract

The Arctic is rapidly melting due to global warming and may experience its first ice free summer in the next 30-40 years. This is regardless of potential emissions reductions unless local preventative action is taken. The loss of Arctic sea ice could lead methane to be released from permafrost, a changing climate in the northern hemisphere as well as a positive feedback loop whereby reduced albedo causes more heat to be absorbed. Preventing the Arctic from melting and perhaps restoring lost ice may help to mitigate the effects of our carbon emissions by increasing the global albedo and thereby reducing global temperature rises. A proposed solution to Arctic melting is to pump seawater on top of existing thin ice in the winter to thicken it and preventing it from melting fully during the warm winter months, also know as ice volcanoes. As the albedo of ice is much greater than that of seawater, more solar radiation is reflected and hence the Arctic is kept cooler helping to prevent more melting. Ice volcanoes and the interaction between water flows and ice have not been researched in depth. The two key pieces of relevant research are an investigation into the feasibility of ice volcanoes with an energy balance over the whole Arctic winter by Desch et al., 2017, and modelling/theory by Cartlidge, 2022 on the response of ice to water flowing down a channel over its surface.

The project follows on primarily from the work of Cartlidge, 2022 repeating the experiments and developing a new model for the channel flow before developing models and conducting experiments for a radial flow. The model and experiments of Cartlidge, 2022 considered a one-dimensional channel rather than a radial flow. However, useful insights were obtained as to how an ice volcano may behave. Firstly, the moment the water first comes into contact with the ice is considered; the temperature at the interface cannot be greater than the phase change temperature, otherwise ice must have melted instantaneously. Similarly it cannot be lower then the phase change temperature as this would imply instantaneous freezing. The interface in both the water and the ice must therefore be the phase change temperature. At the instant the water first touches the ice there is an infinite temperature gradient in the ice at the interface as there has been no time for heat conduction through the ice. Heat convection to the ice is proportional to the temperature difference between the water and the interface and is therefore finite, the difference between the heat fluxes determines the rate of melting/freezing. Therefore, for any (finite) water temperature, the initial response is freezing at an infinite rate. The temperature profile in the ice then weakens as heat is conducted into it and it warms up, meanwhile the heat transfer from the water is constant (as it is flowing over the surface). Hence, after a period of time the newly formed and then the original ice begin to melt. Melting occurs first where the water is injected due to the water being warmest there and then progresses as the temperature profile in the ice continues to weaken. Implications for the ice volcano are clear; if water greater than phase change temperature is pumped continually then the ice volcano shall melt a hole around itself, quickly rendering it useless. It may be possible to avoid this by using water at or very close to phase change temperature (though this presents challenges of its own) or by pumping the onto an artificial solid surface so the water is cooled to phase change temperature by convection to the air. It is also worth noting that convection to the air and radiation are neglected as they are relatively small at the short time scales considered (of the order of minutes); these would beneficially increase heat transfer away from the water.

Two models had been developed previously to predict the change in ice thickness along the channel and a third was developed during the project which provides the most accurate results when compared to experimental data. The first of the theories developed initially assumes that there is no thermal boundary layer in the water and hence a single, bulk temperature decreasing along the length of the channel. The second model assumes instead that there is a thermal boundary layer growing with the square root of the distance along the channel. The new model instead assumes the thermal boundary layer is growing with the cube root of distance, and is the most accurate.

The experiments were carried out in a walk-in freezer at -18°C. An initial layer of ice was frozen in the channel and the depth measured. Water of various temperatures was then pumped on top and allowed to flow down the surface for a period of time before the depth was measured for a second time. These experiments used thermocouples connected to a Raspberry Pi to measure the water temperature flowing down the channel. Previously, this temperature had been assumed to be that of the fridge where the water was stored. However, the results were not reliable when the experiment was repeated without measurement of the water temperature. With measured 0.5 and 0.8°C water supplied to the ice the data was accurately predicted by the new boundary layer theory ($\delta \propto \sqrt[3]{\text{distance}}$). For these temperatures, almost all of the data was bounded by the lower predicted growth of the previous boundary layer model ($\delta \propto \sqrt{\text{distance}}$) and the higher predicted growth of the no boundary layer model. For 2.0°C water the models were less accurate; potential causes of this are inaccurate temperature measurement or a breakdown of the semi-infinite ice depth assumption. The latter is more likely as there was significant melting through most of the ice, especially at the channel inlet where the models deviated the furthest. Water overflowing from the melted region rather than flowing over the ice in a thin film as assumed would also lead to a breakdown of the assumptions in the model.

The experiments undertaken for radial flow matched closely to the two models developed to predict the resulting ice profile. In the first experiment, it is thought that leaving the chest freezer lid open during the experiment led to the water cooling less than expected and hence the water was supplied at a warmer temperature than intended. This shows the difficulty in accurately knowing the temperature when it could not be measured directly. These models are equivalent to the first two models for the channel flow; they consider the flow to be inviscid with either no thermal boundary layer or one growing as the square root of distance. The boundary layer model most accurately predicted the ice growth for the radial flow with both the melting and freezing estimated well apart from very close to the inlet. At the centre of the ice disk the models break down as the water is not injected as a point source, but from a pipe with finite area.

The experiments for both the channel and radial flows show that it is possible to predict the ice profile resulting from water flowing over its surface, though the complex interaction of melting and freezing is challenging to predict. The results and models show that ice volcanoes using greater than phase change temperature water shall not be successful unless action is taken to prevent melting where the water is injected. The report concludes with areas of further research that are required to understand whether ice volcanoes could be used to refreeze the Arctic and the implications of doing so.

Contents

1 Introduction

1.1 Arctic Sea Ice Melting

The extent covered of the Arctic covered by ice has reduced by over 40% since 1979 whilst the volume of ice has reduced by over 70% in the same amount of time (Dunne, 2022). Arctic melting is the result of global warming and it is likely that there shall be an ice-free Arctic summer by 2060 (Dunne, 2022) even if our greenhouse gas emissions significantly reduce. The IPCC, 2018, "has *high confidence*" of overshooting 1.5°C even if current Nationally Determined Contributions are supplemented with "very challenging increases in the scale and ambition of mitigation after 2030". Therefore, it would appear that overshoot is the most optimistic scenario. Overshoot results in an around 80% chance of a summer being ice-free before 2060 and if temperatures are to reach 2°C then this rises to 90% (Dunne, 2022).

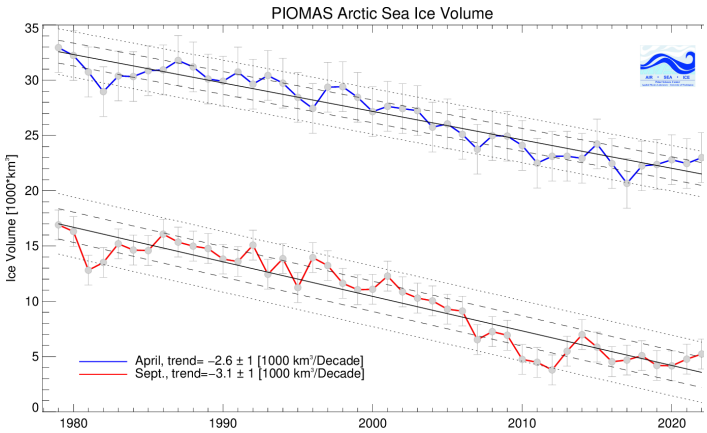

Figure 1: PIOMAS Arctic Ice Volume (Schweiger et al., 2011)

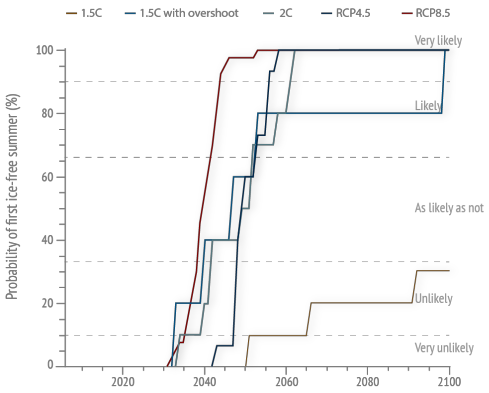

Figure 2: Ice-Free Summer Probability (Dunne, 2022)

Sea ice melting is increased by Arctic amplification; increased temperatures cause ice to melt. This exposes seawater which has an albedo less than a tenth of that of ice (and a fifteenth of that of snow-covered ice, Desch et al., 2017). Hence the area absorbs more solar radiation and heats up. The warmer waters then melt more ice thereby exposing more sea in a positive feedback loop; this is the main driver of Arctic amplification which is causing the region to heat up four times faster than the global average (Rantanen et al., 2022). However, the feedback loop can also work in reverse; if the amount of ice is increased then less solar radiation shall be absorbed and temperatures shall decrease. Desch et al., 2017 calculated that losing all the ice historically present (around 6 million km^2) would result in an increase of energy absorbed by the Arctic equal of almost 3×10^{11} J. Averaged across the globe during a year this is 0.17 Wm^{-2}, which is equivalent to over 14% of anthropogenic radiative forcing. The Arctic melting would therefore cause global temperatures to measurably increase. Alongside increasing global temperatures by a reduction in global albedo, loss of Arctic sea ice leads to increased coastal erosion in Arctic regions, intensification of extreme weather events (from snow storms to droughts) and the release of unknown quantities of methane and CO_2 currently trapped in permafrost (Moon et al., 2019).

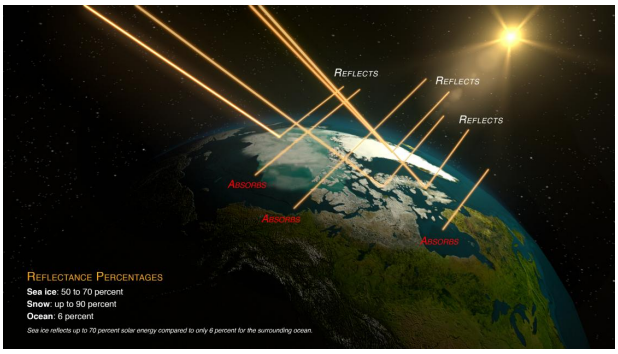

Figure 3: Arctic Albedo
(National Snow and Ice Data Center, n.d.)

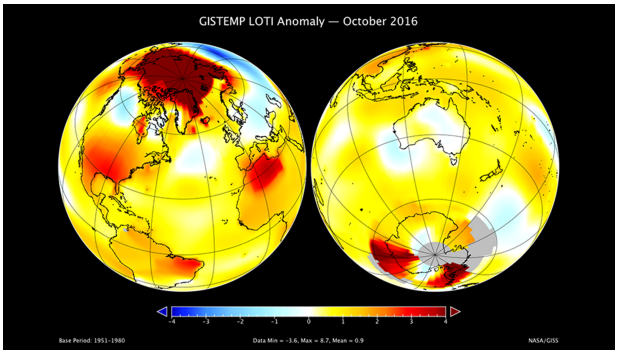

Figure 4: Arctic Amplification
(Goddard Institute for Space Studies, 2016)

Not only has the extent of Arctic ice significantly reduced but the average thickness has halved since records began in 1979 (Desch et al., 2017). Ice that has survived multiple summers, known as multi-year ice, is thicker and stronger than first-year ice so the reduction in the thickness of ice is a concern. Not only is multi-year ice thicker but it also slowly rejects salt in the form of brine; this makes the ice more resistant to melting and to being broken up by waves. Figure 5 shows how the age/thickness of Arctic ice has reduced over the last forty years. The thinning of the ice makes it susceptible to melting more quickly so we must urgently take action to prevent it.

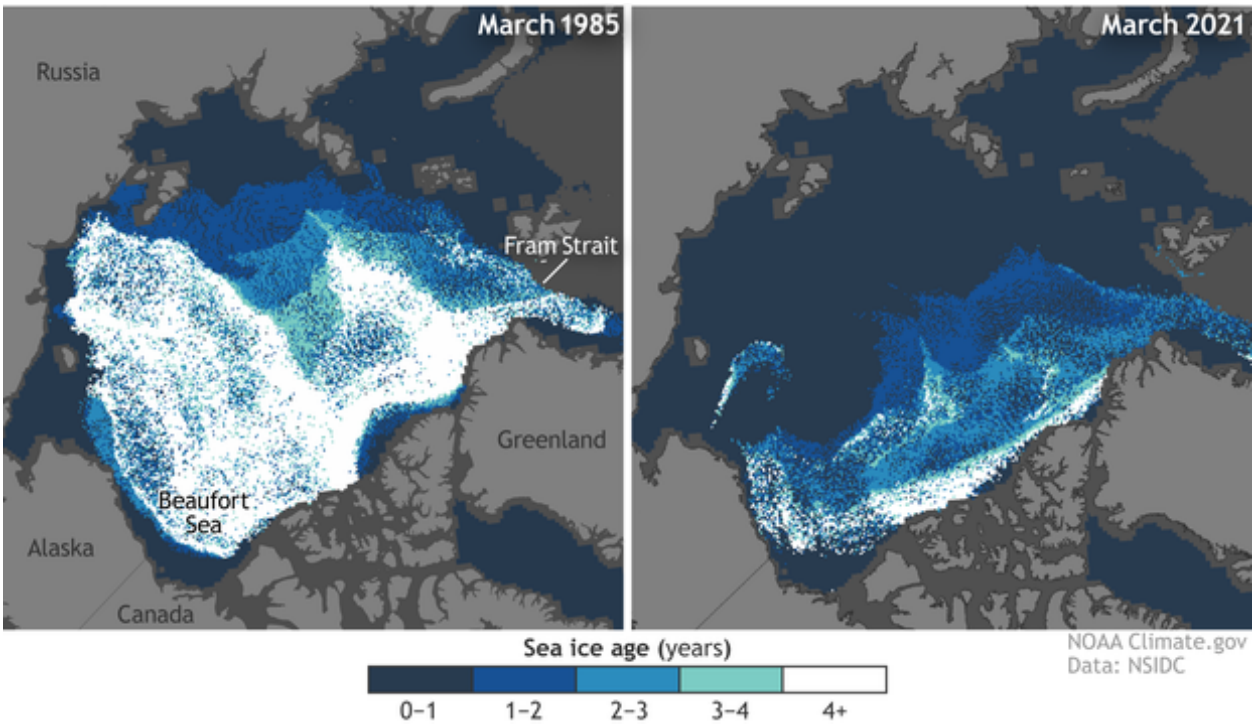

Figure 5: Arctic Ice Thinning (Lindsey and Scott, 2020)

1.2 Ice Thickening through Ice Volcanoes

There are several proposed methods of increasing Arctic ice; these range from scattering reflective beads across the surface of the ice to increase its albedo to marine cloud brightening to reduce the amount of solar radiation. Ice volcanoes are a proposed method of directly increasing the amount of ice that freezes during the winter by pumping water on top of existing ice. Water freezing on the bottom of the ice requires the latent heat to be conducted through the ice and then convected to the air or radiated into space. For new ice that is not forming on exposed water, existing ice is an insulating layer between the water underneath and the cooling that is provided from above. Therefore, if water is pumped on top of the ice it may freeze more quickly thereby thickening the ice and allowing it to survive longer during the summer months. Ice that is thicker than 1.5 m is likely to survive the summer in many areas thereby increasing the albedo and reducing the amount of energy absorbed (Desch et al., 2017).

The proposed ice volcanoes would pump water up and on top of thin ice in the winter, and as it then flows outwards the water would freeze and thicken the ice. Over the whole Arctic winter the ice would be thickened such that it should survive the summer melting. The following year the ice would thicken again and hence become multi-year ice. The exact thickness of ice required will vary across the Arctic region due to meteorological conditions and increased solar radiation at lower latitudes. Desch et al., 2017 calculated that thickening ice by around 1 m would have a significant impact. Their calculations suggested that it would be possible for convection and radiation of heat to provide the necessary cooling to freeze ice to the necessary thickness. However, due to the heat release from water freezing on top of the ice, natural freezing on the bottom of the ice is reduced. The effect is that only 70% of the expected increase in ice is observed, therefore around two fifths of the water that is pumped does not contribute to a net increase in ice. The calculations performed by Desch et al., 2017 only consider a heat balance across the whole of the Arctic summer and they do not calculate the impact of the heat release on the existing ice.

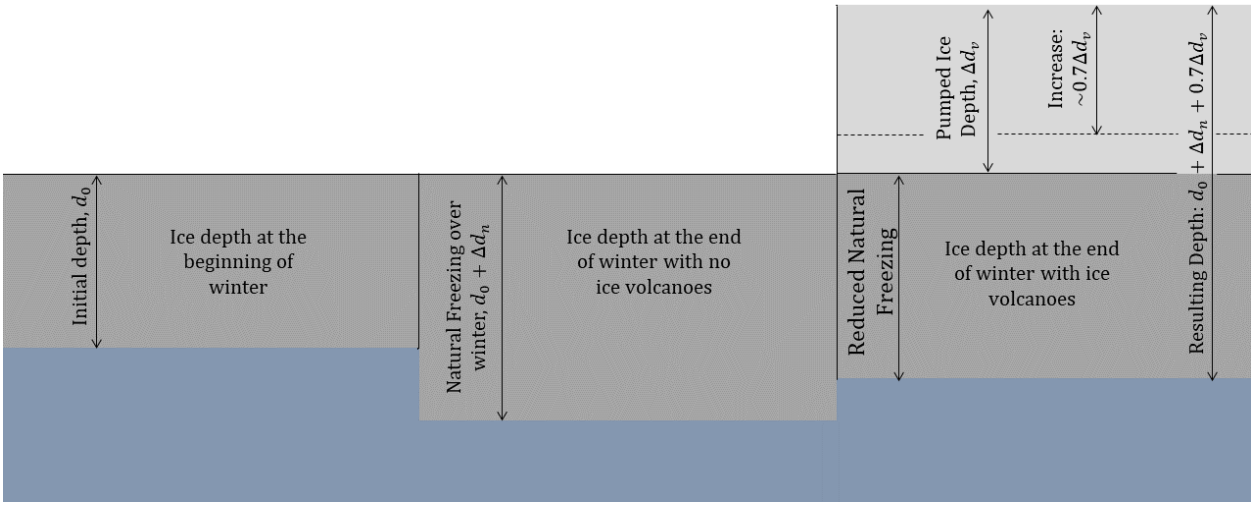

Figure 6: Potential Arctic Ice Growth
(Original Diagram Based on the Calculations of Desch et al., 2017)

Despite the calculations of Desch et al., 2017, there has been very little experimental work or modelling of ice volcanoes themselves. Cartlidge, 2022 performed experiments for water flowing over an ice surface down a channel in a simplified two-dimensional model of an ice volcano. The work showed that an ice profile along the channel could be measured for water injected above its freezing temperature, although these experiments were not repeated. Experiments were also conducted using freezing temperature water; in these experiments the models developed underestimated the measured growth by around 50%. These experiments were conducted in a channel metre long and over time periods of the order of 10 minutes. When these experiments were repeated the results were not reliable. This was thought to be as the result of variations in the water temperature flowing over the ice. This project implements rigorous experiments to obtain data for the case of a channel flow as well as developing a new, more accurate model of the resulting ice profile. The experiments and modelling are then extended to a radial three-dimensional case which is more representative of an ice volcano. The results of the project are presented along with implications for the design and deployment of ice volcanoes and some of the challenges which may arise.

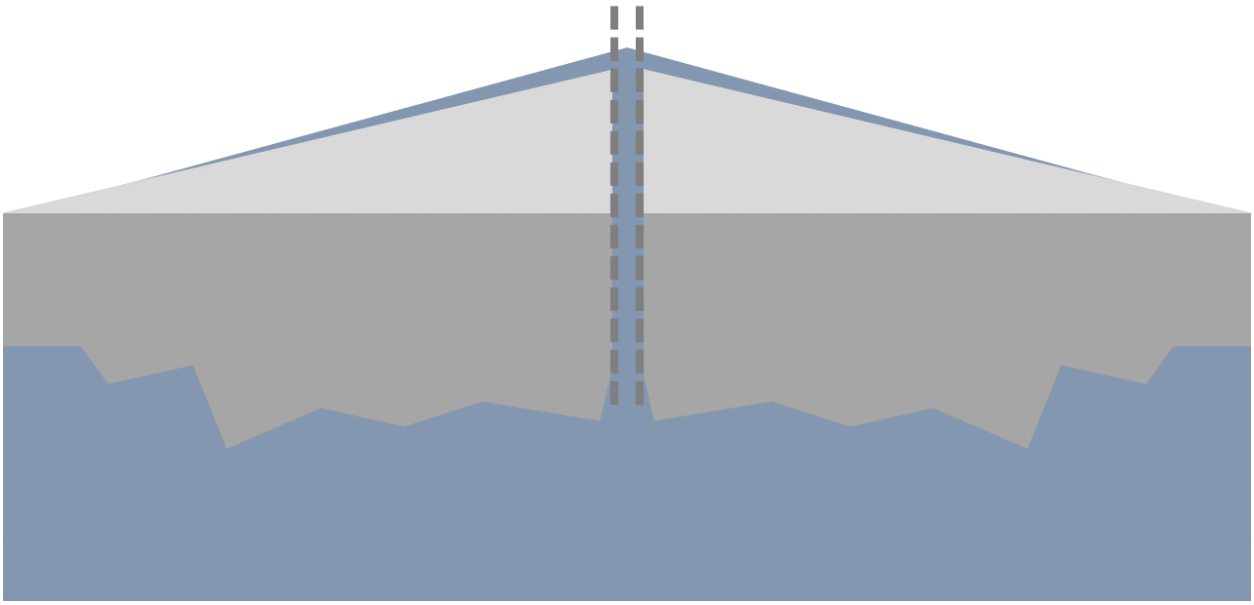

Figure 7: Ice Volcano Concept

2 Modelling

2.1 Previous Modelling

The modelling work done by Cartlidge, 2022 used *Phase changes following the initiation of a hot turbulent flow over a cold solid surface* (Huppert, 1989) as a basis and is derived again here for completeness and as a starting point for further derivations. The assumptions and methods are also used in the derivation of the updated model for the channel case and in the models for the radial case. The ice is taken to be of semi-infinite thickness and cooling due to convection, radiation or evaporation from the water to the atmosphere is neglected. The validity of these assumptions for the time and length scales used are analysed later in this section. Any heat transfer to the walls of the channel is also neglected; experimental results suggest this assumption may be not be valid and this is discussed in the results section.

2.2 Nomenclature

Thermal diffusivity of ice, $\alpha_\mathrm{i} = 1.18 \times 10^{-6}$ m^{2}s^{-1}
Thermal diffusivity of water, $\alpha_\mathrm{w} = 0.132 \times 10^{-6}$ m^{2}s^{-1}
Thermal conductivity of ice, $\lambda_\mathrm{i} = 2.22$ Wm^{-1}K^{-1}
Thermal conductivity of water, $\lambda_\mathrm{w} = 0.56$ Wm^{-1}K^{-1}
Density of ice, $\rho_\mathrm{i} = 916.2$ kgm^{-3}
Density of water, $\rho_\mathrm{w} = 1000$ kgm^{-3}
Specific heat capacity of ice, $c_{p,i} = 2100$ Jkg^{-1}K^{-1}
Specific heat capacity of water, $c_{p,w} = 4200$ Jkg^{-1}K^{-1}
Heat transfer coefficient between water and ice, $h = 2757$ Wm^{-2}K^{-1}
Latent heat of fusions of water, $L = 334,000$ Jkg^{-1}
Phase change temperature of water, $T_\mathrm{pc} = 0$°C

Distance along the channel, x
Perpendicular distance from the initial slope, z
Time since water injection, t
Position of the water-ice interface, $\eta(x,t)$
Temperature of the ice, $T_\mathrm{i}(x,z,t)$ for $z \leq \eta$
Temperature of the water, $T_\mathrm{w}(x,z,t)$ for $z \geq \eta$
Velocity of the flow in the x-direction (assumed constant), v
Depth of the flow (assumed constant), d
Small angle of the slope to provide steady flow, ϕ
Conductive heat flux through the ice, q_ice
Convective heat flux from the water to the ice, q_water
Latent heat flux from water freezing, q_latent

Note that where a parameter is dependent on various positions in space and time the convention of $f(x,z,t)$ shall be followed. For example $T_\mathrm{i}(0,\eta,0^+)$ represents the temperature of the ice at the channel inlet ($x = 0$), at the interface ($z = \eta$), instantaneously after the water is injected ($t = 0^+$). It should also be noted that figures include plots with various colours representing different times, positions, models or temperatures; different colour schemes have been used in each of the four cases.

3 Modelling - Channel Flow

3.1 Setting Up the Problem

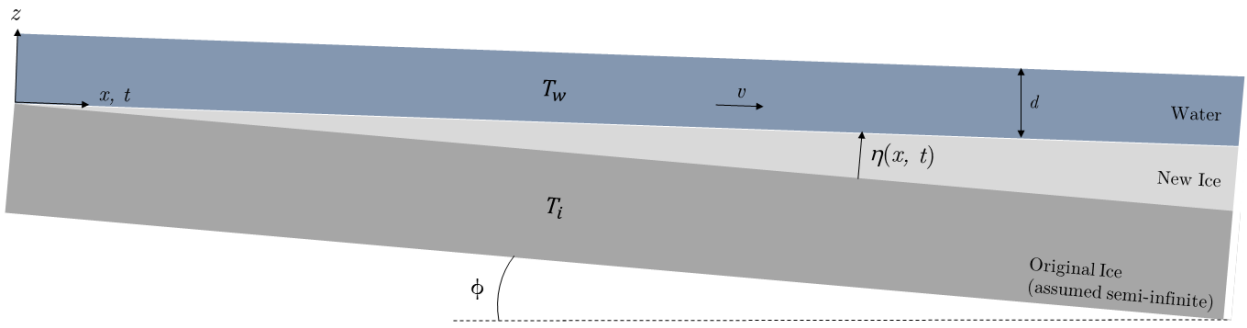

Figure 8: Theoretical Model of Water Flowing Down a Channel Over Semi-Infinite Ice

Shown in Figure 8 is the setup for deriving the development of the ice profile for the case of water flowing along its surface down a channel. The water enters the channel at $x = 0$ with temperature T_{w0} and then flows down the surface with a gravity driven velocity v and depth d. The change in the depth of ice, η, may be positive or negative as a result of either water freezing or ice melting. The mass flow of ice to water or water to ice is assumed to be much smaller than the flow rate of the water injected and this is therefore assumed to be constant. The ice is assumed to be semi-infinite such that the temperature signal does not fully penetrate the ice during the experiment; this assumption is verified later. The model simplifies the ice volcano greatly by limiting it to a two dimensional slice. The water depth does not vary along the length of the channel (whereas it decreases in the radial case). The channel flow provides basic insights into how the complicated ice volcano may progress. The inclination of the channel, ensures that the water flows down the channel, although this shall not be present in the radial case. As the angle of inclination, ϕ, is small it shall be ignored henceforth in both diagrams and analysis. In all the following diagrams the vertical axis represents the the vertical position (with respect to the initial ice surface). The horizontal axis represents various parameters including distance along the channel, ice depth and time.

Heat transfer to the atmosphere by convection and radiation are neglected over short time scales when compared to the convection through and the conduction to the ice (this is verified at the end of the section). Therefore, there are only two mechanisms for heat transfer that need to be considered; the first is the convection of heat from the water to the ice q_{water}, which will cool the water and warm/melt the ice. The second is the conduction of heat through the ice, q_{ice}, which will transfer heat from the surface deeper into the ice. The freezing of water will release latent heat and similarly the melting of ice will absorb latent heat. The difference between the heat conducted away from the interface and the heat convected to it will determine whether there is freezing or melting.

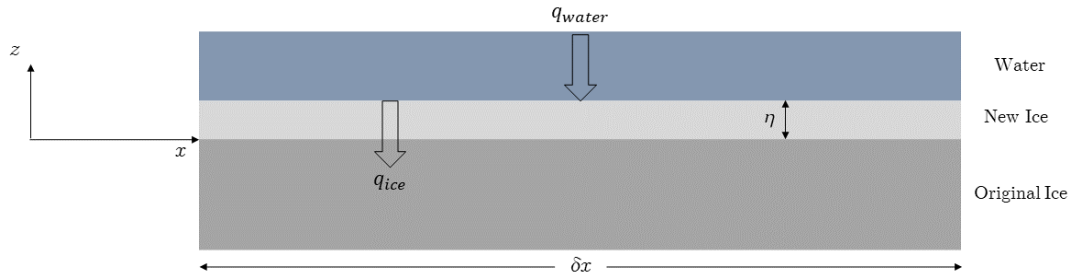

Figure 9: Heat Transfers in the System

The heat flux through the ice shall be proportional to the temperature gradient in the ice. The flux at the interface, q_{ice}, will therefore be proportional to the local temperature gradient at the interface. The interface is defined as at $z = \eta$ where η is the change in ice depth, therefore:

$$q_{\text{ice}}(x,t) \propto \left.\frac{\partial T_{\text{i}}}{\partial z}\right|_{z=\eta} = \lambda_{\text{i}} \left.\frac{\partial T_{\text{i}}}{\partial z}\right|_{z=\eta}$$

Where λ_{i} is the thermal conductivity of ice and T_{i} is the temperature of the ice which may vary in both space and time (x, t).

The heat flux from the water to the ice interface shall be proportional to the temperature difference between the water and the interface which may be characterised by various assumptions discussed in the next section:

$$q_{\text{water}}(x,t) \propto (T_{\text{w}} - T_{\text{interface}}) = h(T_{\text{w}} - T_{\text{pc}})$$

Where h is a heat transfer coefficient between the water and ice, T_{w} is the temperature of the water, which may vary in space and time and $T_{\text{interface}}$ is the temperature of the interface. The temperature of the interface is required to be the freezing/melting temperature of water/ice as explained below.

3.2 Initial Behaviour at the Interface

Before coming into contact with one another the water is at a constant temperature, T_{w0} greater than or equal to the phase change temperature. Similarly, the ice is initially at a temperature, T_{w0} less than or equal to the phase change temperature. At the instant the water first comes into contact with the ice $(t = 0^{+})$, there must immediately be a continuous temperature profile across the interface. The temperature at the interface cannot be below the phase change temperature otherwise water must have instantly frozen. Similarly, if the interface temperature exceeded the phase change temperature this would mean that some ice had immediately melted. Huppert, 1989 identified that the interface temperature must be equal to the phase change temperature for any position and time:

$$T_{\mathrm{i}}(x,\eta,t) = T_{\mathrm{w}}(x,\eta,t) = T_{\mathrm{pc}}$$

The ice is at a temperature $T_{\mathrm{i}0}$ for $z \leq 0$ and $t < 0$. Instantaneously there has not been time for freezing/melting (i.e. $\eta = 0$) therefore the ice surface must immediately be at the phase change temperature when the water comes into contact with it at $t = 0^{+}$: $T_{\mathrm{i}}(x,0,0^{+}) = T_{\mathrm{pc}}$. At the instant when the water comes into contact with the ice, there has also been no time for heat transfer so the ice temperature just below the surface must be the initial ice temperature: $T_{\mathrm{i}}(x,0^{-},0^{+}) = T_{\mathrm{i}0}$. This result is shown in Figure 10.

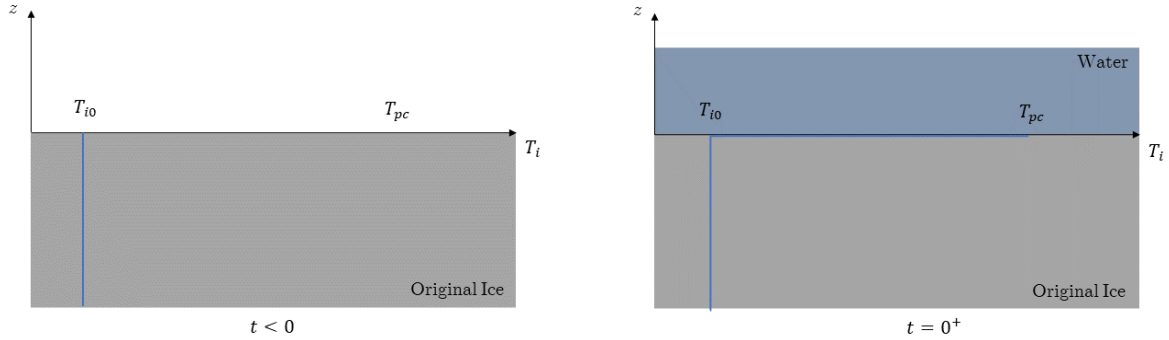

Figure 10: Water-Ice Interface Condition at $t = 0^{+}$

The temperature gradient in the ice at the interface just after contact with the water tends to infinity as there is a step change in the temperature of the ice. As the conductive heat transfer is proportional to this temperature gradient must also tend to infinity at the interface:

$$\left.\frac{\partial T_{\mathrm{i}}}{\partial z}\right|_{z=\eta} \to \infty \qquad (t = 0^{+}): \qquad q_{\mathrm{ice}} = \lambda_{\mathrm{i}} \left.\frac{\partial T_{\mathrm{i}}}{\partial z}\right|_{z=\eta} \to \infty \qquad (t = 0^{+})$$

The conductive heat flux must be balanced by the convection from the water to the ice and the latent heat of freezing/melting. The convection is proportional to the finite temperature difference between the water and interface and therefore the initial infinite heat conduction through the ice (away from the interface) must be balanced by an infinite rate of freezing. This condition is true for any (finite) water temperature leading to the perhaps unexpected result that whenever water comes into contact with ice the immediate response shall be freezing at an infinite rate. The initial behaviour of the ice-water system was previously identified by Huppert, 1989. Although the instantaneous response is an infinite rate of freezing, the heat is then conducted into the ice, weakening the temperature gradient and therefore reducing the rate of heat transfer.

3.3 Development of the Ice Profile

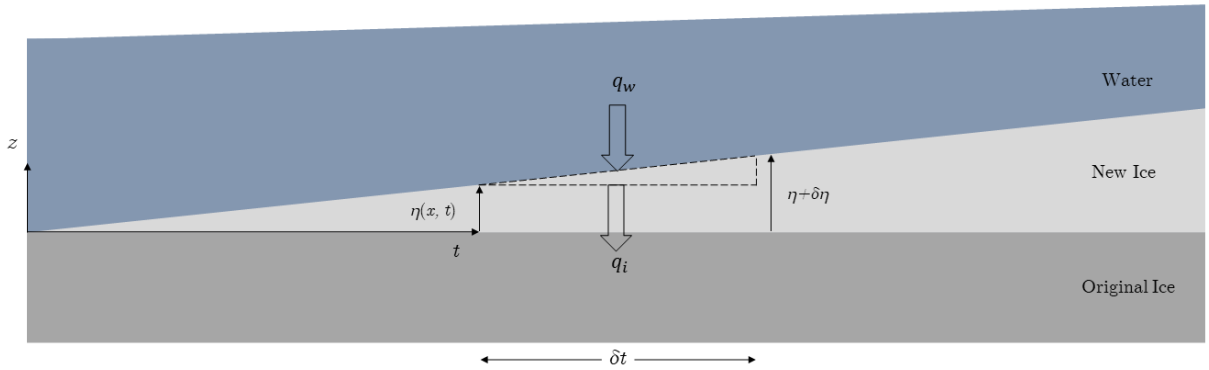

Figure 11: Control Volume at Interface for the Channel Case

The heat fluxes and the release/absorption of latent heat can be analysed analytically to predict how the ice profile develops beyond the initial response. Figure 11 shows a control volume around a section of ice growth over a period δt, with heat convection from the water to the control volume and heat transfer from the control volume through the ice. The latent heat released per unit area of freezing is $\rho_\mathrm{i} L \delta\eta$, therefore by applying the energy conservation:

$$q_\mathrm{water}(x,t)\delta t + \rho_\mathrm{i} L \delta\eta(x,t) - q_\mathrm{ice}(x,t)\delta t = 0$$

$$\rho_\mathrm{i} L \frac{\partial \eta}{\partial t} = q_\mathrm{ice} - q_\mathrm{water}$$

Where $\frac{\partial \eta}{\partial t}$, q_ice and q_water may be functions of both time and space (x,t). This result was previously derived by Cartlidge, 2022 with slightly different notation. Substituting the equations for the heat transfer from the water and to the ice gives:

$$\rho_\mathrm{i} L \frac{\partial \eta}{\partial t} = \lambda_\mathrm{i} \left.\frac{\partial T_\mathrm{i}}{\partial z}\right|_{z=\eta} - h(T_\mathrm{w} - T_\mathrm{pc})$$

The above equations can be used to qualitatively discuss the ice growth; when/where the heat conduction exceeds the heat convection there will be ice freezing. This is expected to occur at short time scales when there has been little time for the temperature gradient to weaken, or far away from the channel inlet where the water will have cooled. When and where the convective heat flux exceeds the conductive heat flux there will be melting as there will be net heat flux to the interface (freezing will occur where there is a heat away from the interface). Melting is therefore expected at long time scales when the ice has reached relatively warm temperatures and close to the channel inlet where convection is be strongest. The development of the ice profile will depend upon the temperatures of both the ice and the water which influence conduction and convection respectively.

3.4 Phase Change Temperature Water

If the water is initially at its phase change temperature it cannot cool any further and hence $T_\mathrm{w}(x,z,t) = T_\mathrm{pc}$, therefore there shall also be no heat convection from the water to the ice. Either the water remains at phase change temperature or it freezes in which case it can then cool further. The rate of freezing is only dependent on the conduction through the ice (as heat transfer to the surroundings is neglected). As the ice and water temperatures are uniform along the length of the channel, the system becomes independent of the position along the channel: $T_\mathrm{i}(x,z,t) = T_\mathrm{i}(z,t)$ and the ice growth can also be expected to be independent of channel position: $\eta(x,t) = \eta(t)$. As the water can only freeze or remain liquid the problem becomes known as the 'one-phase Stefan problem' since the water phase can be neglected. For phase change temperature water the equation for ice growth becomes:

$$\rho_\mathrm{i} L \frac{\partial \eta}{\partial t} = \lambda_\mathrm{i} \left.\frac{\partial T_\mathrm{i}}{\partial z}\right|_{z=\eta}$$

This can be coupled with the heat diffusion equation for the temperature of the ice which only varies along the vertical (z) axis:

$$\frac{\partial T_\mathrm{i}}{\partial t} = \alpha_\mathrm{i} \frac{\partial^2 T_\mathrm{i}}{\partial z^2}$$

These equations were solved by Cartlidge, 2022 who modelled the ice growth as a function of time. Two models of the ice growth were considered, the first ignores the small change in the location of the interface between the ice and water as some of the water freezes. The interface in the model is assumed to remain constant at $z = 0$ rather than being modelled as at the true ice height $z = \eta$. As the interface moves upwards the heat shall have to conduct further to reach T_i0 far away from the interface, therefore this model predicts a steeper temperature gradient from T_pc to T_i0 hence an overestimate of the freezing is expected. The ice growth in this model is directly proportional to the difference between the initial ice and phase change temperatures and grows with the square root of time. The equation for the ice growth ignoring the contribution of the moving interface is as follows:

$$\eta_\mathrm{st}(t) = \frac{2c_\mathrm{p,i}(T_\mathrm{pc} - T_\mathrm{i0})}{\sqrt{\pi} L} \sqrt{\alpha_\mathrm{i} t}$$

The model including the moving interface is more complex and must be solved numerically as an iterative solution for the parameter γ must be found. The ice growth no longer depends directly upon the temperature difference, though the growth is still proportional to the square root of time. The following equations describe the ice growth for the model including the contribution of the moving interface:

$$\eta_\mathrm{mov}(t) = 2\gamma\sqrt{\alpha_\mathrm{i} t}, \qquad \gamma = -\frac{c_\mathrm{p,i}(T_\mathrm{i0} - T_\mathrm{pc})}{\sqrt{\pi} L} \frac{\exp\left(-\gamma^2\right)}{1 + \mathrm{erf}\left(\gamma\right)}$$

Alternatively:

$$\eta_\mathrm{mov}(t) = \gamma' \eta_\mathrm{st}(t), \qquad \gamma' = \gamma \Bigg/ \frac{c_\mathrm{p,i}(T_\mathrm{i0} - T_\mathrm{pc})}{\sqrt{\pi} L}$$

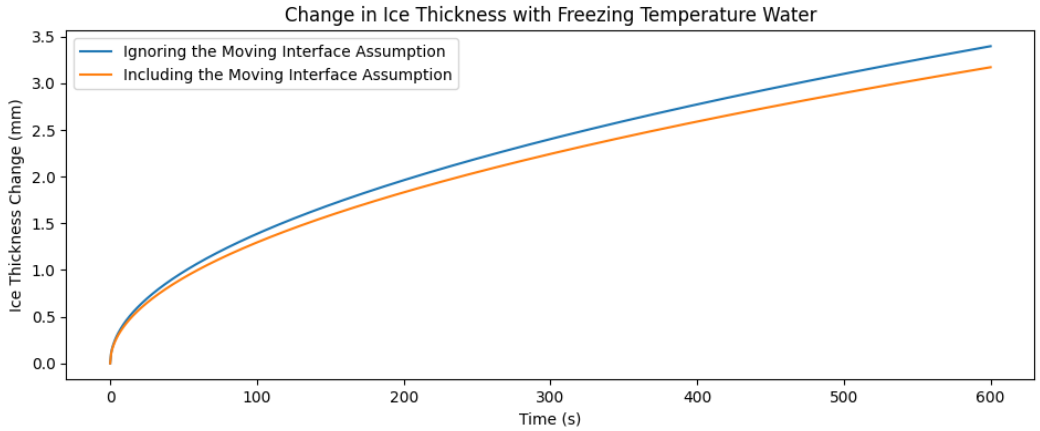

Figure 12: Ice Growth with Phase Change Temperature Water

The two models describing the development of the ice profile with phase change temperature water are shown in Figure 12. These diverge slightly at longer time scales (when the ice growth is larger). However, the difference is relatively small for the time scales of interest. The percentage difference is time invariant and for ice of -18°C is less than 7% between the two models. Figure 13 shows the value of γ' with increasing temperature difference (i.e. decreasing initial ice temperature). As expected, at lower initial ice temperatures, there is a larger discrepancy between the two models, this is due to the larger temperature difference acting over the same difference in the position of the interface. At the temperatures of interest it is assumed henceforth that the moving interface can be neglected and that heat transfer occurs at $z = 0$. This assumption is challenged later in the analysis of experiments for warmer than phase change temperature water.

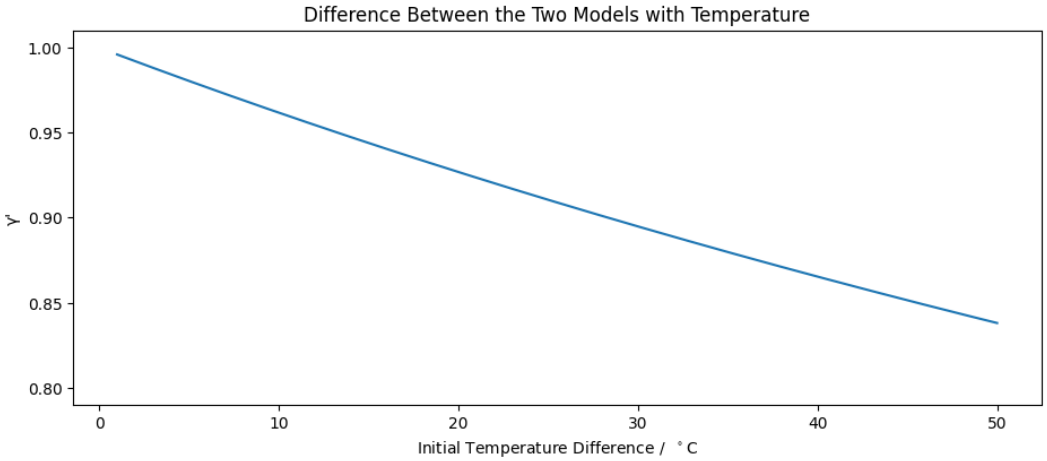

Figure 13: Difference Between Ignoring and Including the Moving Interface

3.5 Above Phase Change Temperature Water

Water above its freezing temperature may freeze or it may cause ice to melt depending upon the balance between the conduction of heat away through the ice and the convection of heat from the water to the ice. When the conduction of heat through the ice exceeds the convection of heat to it then freezing will occur. Similarly, if the conduction is exceeded by the convection then there will be melting, this is shown in Figure 14.

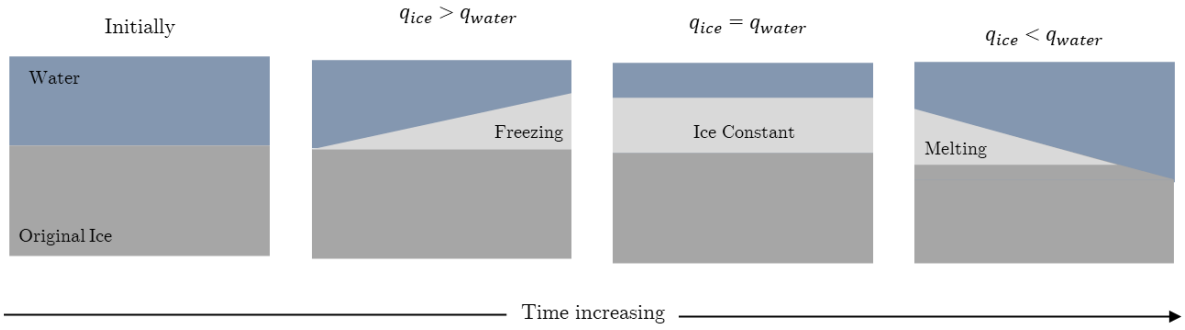

Figure 14: Impact of Relative Magnitudes of Conduction and Convection

The water now enters at an initial temperature greater than the phase change temperature, $T_{\mathrm{w}}(0,z,t) = T_{\mathrm{w0}}$. The interface temperature will still be equal to the phase change temperature and there shall be an initial infinite rate of freezing. However, as the water can now cool as well as freeze the behaviour of the system is very different. Firstly, the temperature profile of the ice must be derived. The heat diffusion equation ($\frac{\partial T_{\mathrm{i}}}{\partial t} = \alpha_{\mathrm{i}} \nabla^2 T_{\mathrm{i}}$) governs the heat transfer through the ice. With a relatively high flow velocity of the water compared to the characteristic velocity of the temperature signal ($v >> \sqrt{\alpha_{\mathrm{i}}/t}$) the variation of temperature along the channel can be neglected, hence:

$$\frac{\partial T_{\mathrm{i}}}{\partial t} = \alpha_{\mathrm{i}} \nabla^2 T_{\mathrm{i}} = \alpha_{\mathrm{i}} \frac{\partial^2 T_{\mathrm{i}}}{\partial z^2}$$

The boundary conditions for the ice are that it is all initially at a uniform temperature, $T_{\mathrm{i}}(x,z,0) = T_{\mathrm{i0}}$. The ice is semi-infinite hence the temperature far away from the interface is still at the initial temperature: $T_{\mathrm{i}}(x,-\infty,t) = T_{\mathrm{i0}}$. Finally, ignoring the moving interface, the temperature at the ice surface is the phase change temperature: $T_{\mathrm{i}}(x,0,t) = T_{\mathrm{pc}}$. The solution of the equation for heat diffusion has the general solution:

$$T_{\mathrm{i}} = A + B \operatorname{erf}\left(\frac{z}{2\sqrt{\alpha_{\mathrm{i}} t}}\right)$$

As $z \to \pm\infty$, $\operatorname{erf}(z) \to 0$, therefore the semi-infinite ice thickness and the initial state boundary conditions are equivalent and lead to:

$$A = T_{\mathrm{i0}}$$

The interface condition is $T_i = T_{pc}$ at $z = 0$ hence $T_{pc} = T_{i0} + B\,\mathrm{erf}(0) = T_{i0} + B$:

$$B = T_{pc} - T_{i0}$$

The equation for the temperature of the ice profile is therefore a function of four parameters; the initial ice temperature, the phase change temperature, the depth into the ice and the time since the water was injected:

$$T_i(z,t) = T_{pc} + (T_{pc} - T_{i0})\,\mathrm{erf}\left(\frac{z}{2\sqrt{\alpha_i t}}\right)$$

The conduction through the ice, q_{ice} is given by $\lambda_i \left.\frac{\partial T_i}{\partial z}\right|_{z=\eta}$, however, ignoring the moving interface has approximated the heat transfer occurring at $z = 0$ rather than $z = \eta$ hence:

$$q_{ice} \approx \lambda_i \left.\frac{\partial T_i}{\partial z}\right|_{z=0}$$

Differentiating the above equation for the temperature in the ice gives:

$$\frac{\partial T_i}{\partial z} = (T_{pc} - T_{i0}) \cdot \frac{2}{\sqrt{\pi}} \cdot \frac{1}{2\sqrt{\alpha_i t}} \cdot \exp\left(\frac{z}{2\sqrt{\alpha_i t}}\right) = \frac{T_{pc} - T_{i0}}{\sqrt{\pi \alpha_i t}} \exp\left(\frac{z}{2\sqrt{\alpha_i t}}\right)$$

Evaluating the equation at $z = 0$ and substituting into the conduction equation:

$$q_{ice} = \frac{\lambda_i (T_{pc} - T_{i0})}{\sqrt{\pi \alpha_i t}}$$

As expected, at $t = 0$ the above equation gives an infinite rate of heat transfer for any (below phase change) initial ice temperature. The rate of conduction decreases over time as the ice near to the boundary gets warmer and the temperature gradient weakens. This result was previously derived by Cartlidge, 2022. The warming of the ice by conduction is shown in Figure 15 for three depths into the ice (measured from the initial surface).

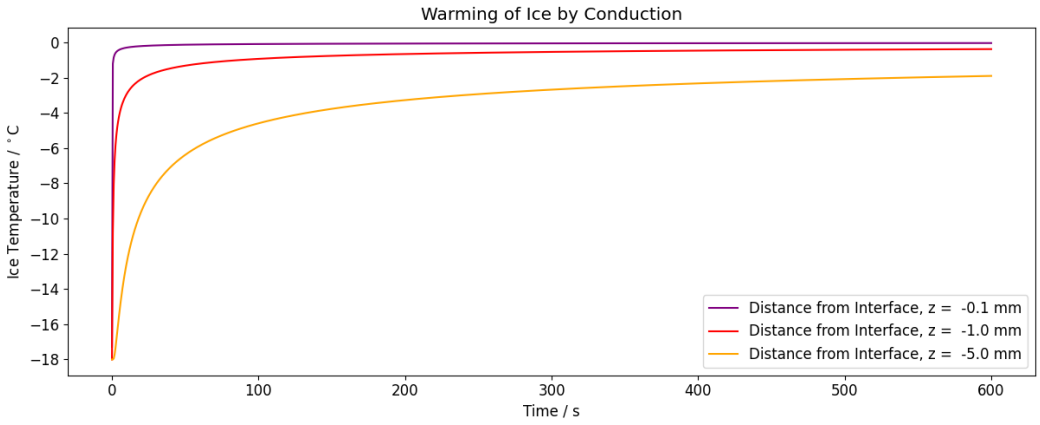

Figure 15: Temperature Through the Ice Over Time

3.5.1 Inviscid Channel Flow with No Thermal Boundary Layer

If the water is assumed to be well mixed then there will be no temperature variation throughout the depth of the water (other than an infinitesimal depth at the interface). The entire depth of the water will have a bulk temperature that will decrease along the channel as shown in Figure 16. As the flow velocity is relatively large compared with the characteristic velocity of conduction in the water (i.e. $v >> \sqrt{\alpha_w/t}$) the water velocity is only affected by the convection and hence is only a function of the position along the channel.

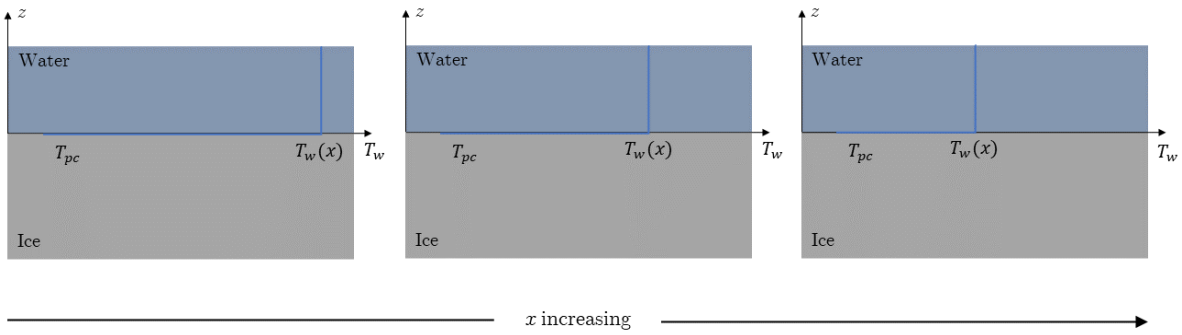

Figure 16: Water Temperature with No Thermal Boundary Layer

The water temperature can be derived by considering the energy balance on the flow at an arbitrary position down the channel; the heat transferred away from the flow by convection must cool the bulk water temperature. The heat transfer by convection for the bulk temperature assumption is $h(T_w - T_{pc})$, where h is a heat transfer coefficient.

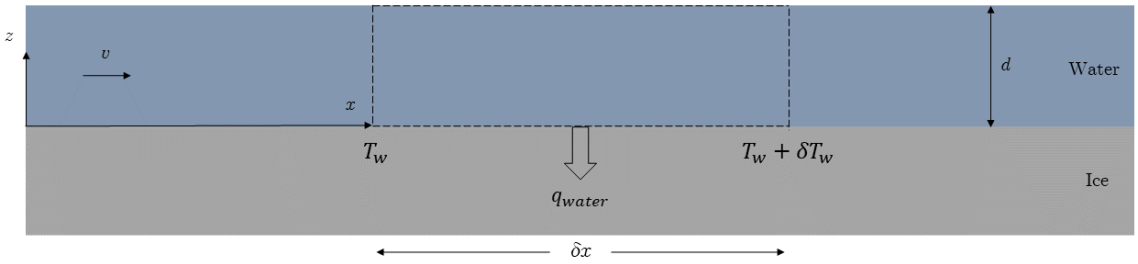

Figure 17: Control Volume for Deriving the Water Temperature Profile

Applying conservation of energy to the control volume (per unit depth into the page), the change in enthalpy of the water must be equal to the heat transferred away from it by convection:

$$\rho_w dv c_{p,w}(T_w + \delta T_w) - \rho_w dv c_{p,w} T_w = -q_{water}\delta x$$

Substituting in for q_{water}, rearranging and taking the limit as $\delta x \to 0$:

$$\rho_{\text{w}} dv c_{\text{p,w}} \frac{dT_{\text{w}}}{dx} = -h(T_{\text{w}} - T_{\text{pc}})$$

T_{pc} is fixed and therefore $d(T_{\text{w}} - T_{\text{pc}})$ is identical to dT_{w}. Using this and rearranging the equation above:

$$\frac{d(T_{\text{w}} - T_{\text{pc}})}{T_{\text{w}} - T_{\text{pc}}} = -\frac{h}{\rho_{\text{w}} dv c_{\text{p,w}}} dx$$

$$\int_{T_{\text{w0}}}^{T_{\text{w}}} \frac{1}{T_{\text{w}} - T_{\text{pc}}} d(T_{\text{w}} - T_{\text{pc}}) = \int_0^x -\frac{h}{\rho_{\text{w}} dv c_{\text{p,w}}} dx$$

$$\ln\left(\frac{T_{\text{w}} - T_{\text{pc}}}{T_{\text{w0}} - T_{\text{pc}}}\right) = -\frac{h}{\rho_{\text{w}} dv c_{\text{p,w}}} x$$

$$T_{\text{w}}(x) = T_{\text{pc}} + (T_{\text{w0}} - T_{\text{pc}}) \exp\left(-\frac{h}{\rho_{\text{w}} dv c_{\text{p,w}}} x\right)$$

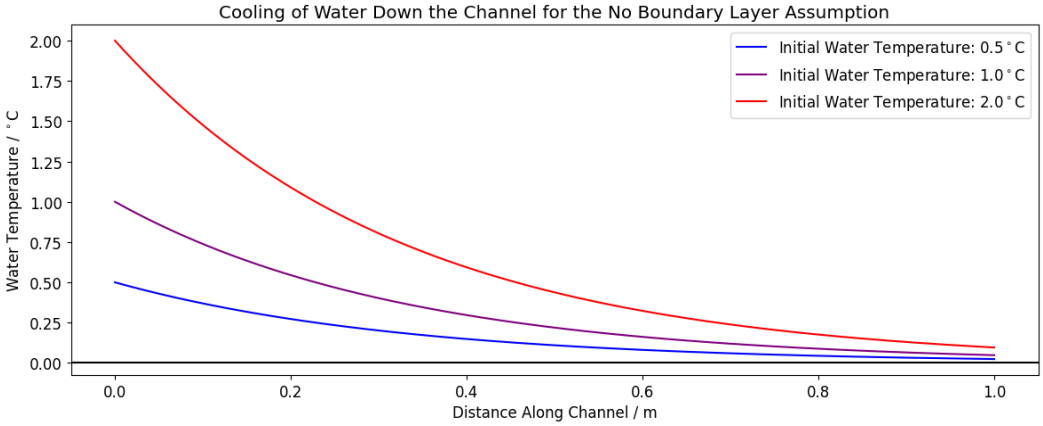

Figure 18: Water Temperatures Down the Channel

The heat transfer by convection is given by $h(T_{\text{w}} - T_{\text{pc}})$ as noted above therefore for the case of a flow with a bulk temperature and no velocity boundary layer the convective heat transfer is:

$$q_{\text{water}} = h(T_{\text{w0}} - T_{\text{pc}}) \exp\left(-\frac{h}{\rho_{\text{w}} dv c_{\text{p,w}}} x\right)$$

This equation can then be substituted into the equation for the rate of ice growth/melting:

$$\rho_{\text{i}} L \frac{\partial \eta}{\partial t} = \frac{\lambda_{\text{i}}(T_{\text{pc}} - T_{\text{i0}})}{\sqrt{\pi \alpha_{\text{i}} t}} - h(T_{\text{w0}} - T_{\text{pc}}) \exp\left(-\frac{h}{\rho_{\text{w}} dv c_{\text{p,w}}} x\right)$$

Integrating this equation to find the change in ice thickness is then trivial and gives the following equation:

$$\eta(x,t) = \frac{1}{\rho_{\text{i}} L}\left(\frac{2\lambda_{\text{i}}(T_{\text{pc}} - T_{\text{i0}})}{\sqrt{\pi \alpha_{\text{i}}}} \sqrt{t} - h(T_{\text{w0}} - T_{\text{pc}}) e^{-\frac{h}{\rho_{\text{w}} dv c_{\text{p,w}}} x} t\right)$$

The progression of the ice profile is shown in Figure 19; for relatively cool water (0.5°C) there is freezing along the length of the channel. With warmer temperatures the convection exceeds the conduction more quickly hence there is melting at the start of the channel and growth further along. At the inlet the difference in the height of ice is over 5 mm for when the temperature increases by a factor of four to 2.0°C, showing the large sensitivity to inlet water temperature as discussed later.

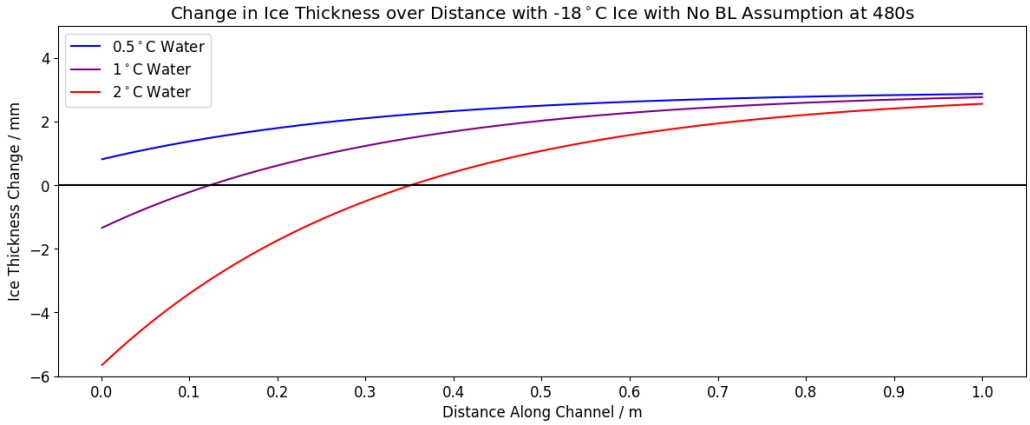

Figure 19: Development of the Ice Profile for the Inviscid No Thermal Boundary Layer Assumption

The normalised difference in heat transfer $(q_{\text{ice}} - q_{\text{water}})/q_{\text{ice}}$ is shown in Figure 20 for three times and 1.0°C water. The horizontal axis marks where the conduction and convection are equal, hence where the rate of change in ice thickness is zero. Above the axis there is freezing with the rate increasing away from the axis, whilst below the axis there is melting. However, as shown, there may be freezing at a location initially and melting at a later time so the graph does not show the net change in ice thickness (as is shown in Figure 19). As the water quickly cools the convection tends to zero, hence the asymptote shown in the figure.

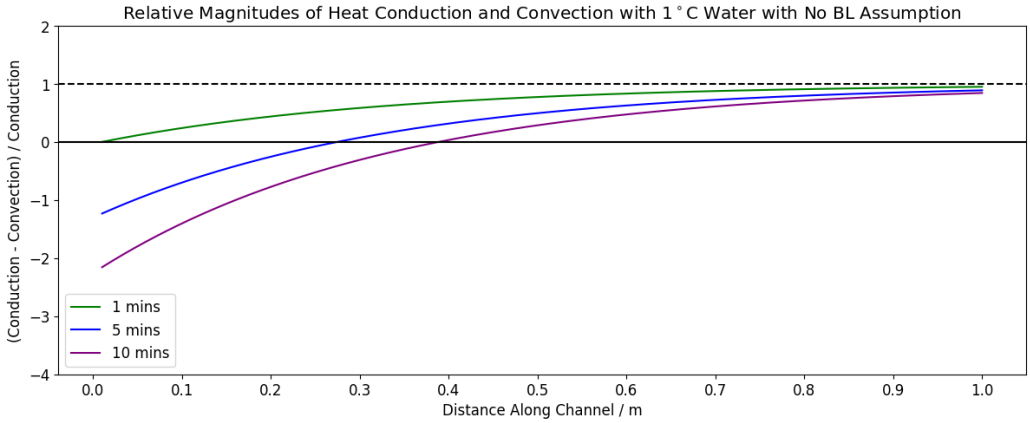

Figure 20: Relative Magnitudes of Conduction and Convection for the NBL Assumption

3.5.2 Inviscid Channel Flow with a Thermal Boundary Layer

For parallel flow the thermal boundary layer equation is as follows:

$$u\frac{\partial T}{\partial x} = \alpha_{\mathrm{w}}\frac{\partial^2 T}{\partial z^2}$$

There are multiple assumptions that could be made about the velocity profile of the water, considered first is the case of a constant (in z) bulk velocity, v. Approximating the temperature changes to be ΔT_0 and taking the thermal boundary layer thickness to be δ:

$$v\frac{\Delta T_0}{x} \sim \alpha_{\mathrm{w}}\frac{\Delta T_0}{\delta^2}$$

Solving for δ, the thermal boundary layer thickness, shows that it grows with $\sqrt{x}$:

$$\delta \sim \sqrt{\frac{\alpha_{\mathrm{w}} x}{v}}$$

The corresponding heat transfer coefficient, h, is given by $\lambda_{\mathrm{w}}/\delta$:

$$h = \lambda_{\mathrm{w}}\sqrt{\frac{v}{\alpha_{\mathrm{w}} x}} \qquad (x > 0)$$

This heat transfer coefficient describes the heat transfer from the bulk flow above the thermal boundary layer (at constant temperature T_{w0}) through the thermal boundary layer to the interface (at temperature T_{pc}). As the thermal boundary layer grows the heat must be transported further and therefore the rate of convection is reduced. The temperature through the thermal boundary layer has not been solved as the temperature difference of importance is that across the thermal boundary layer (ΔT_0 above). The heat transfer by convection from the water is now given by:

$$q_{\mathrm{water}} = \lambda_{\mathrm{w}}(T_{\mathrm{w0}} - T_{\mathrm{pc}})\sqrt{\frac{v}{\alpha_{\mathrm{w}} x}}$$

The equation for the convective heat transfer through the $\sqrt{x}$ thermal boundary layer can now be substituted into the equation for the rate of ice thickness change which can again be integrated to obtain:

$$\rho_{\mathrm{i}} L\frac{\partial \eta}{\partial t} = \frac{\lambda_{\mathrm{i}}(T_{\mathrm{pc}} - T_{\mathrm{i0}})}{\sqrt{\pi \alpha_{\mathrm{i}} t}} - \lambda_{\mathrm{w}}(T_{\mathrm{w0}} - T_{\mathrm{pc}})\sqrt{\frac{v}{\alpha_{\mathrm{w}} x}}$$

$$\eta(x,t) = \frac{1}{\rho_{\mathrm{i}} L}\left(\frac{2\lambda_{\mathrm{i}}(T_{\mathrm{pc}} - T_{\mathrm{i0}})}{\sqrt{\pi \alpha_{\mathrm{i}}}}\sqrt{t} - \lambda_{\mathrm{w}}(T_{\mathrm{w0}} - T_{\mathrm{pc}})\sqrt{\frac{v}{\alpha_{\mathrm{w}} x}}\, t\right)$$

The ice profile shown in Figure 21 develops very differently compared to the no thermal boundary layer assumption; the convective ice heat transfer close to the channel inlet is very large as the thermal boundary layer is very thin close to the inlet. As the convective heat transfer is proportional to $1/\sqrt{x}$ it decreases much more slowly than the previous exponential model, hence there is melting all the way down the channel for 2.0°C water. The net change in the volume of ice even for 1°C is also negative which implies ice volcanoes would not be feasible.

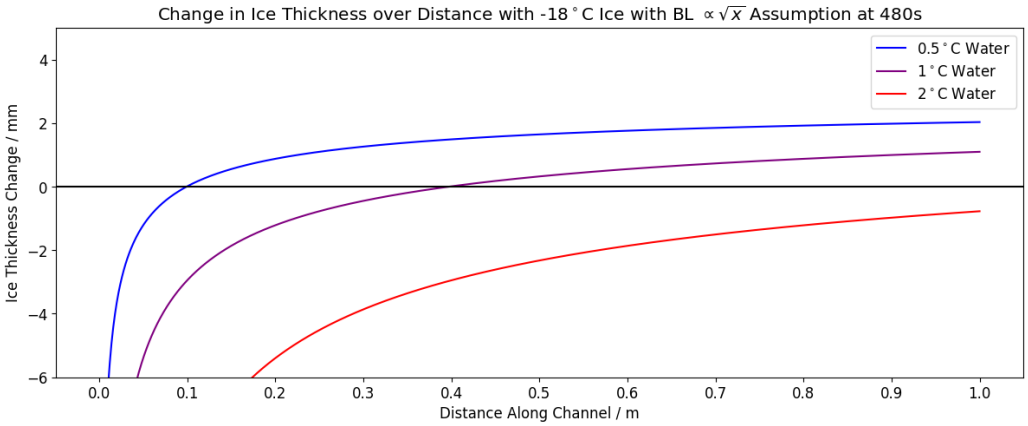

Figure 21: Development of the Ice Profile for the $\delta \propto \sqrt{x}$ Assumption

The difference in heat transfer between the conduction through the ice and convection from the water confirms what is shown in Figure 21. Figure 22 shows how the convection quickly exceeds the conduction all the way down the channel after around ten minutes. The melting that occurs shall then destroy any ice that had built up and then the original ice according to this model. As with the ice profiles, the convective heat transfers do not reduce as quickly to converge at the asymptote on the plot. The graph shows that in the case of water with a thermal boundary layer growing with $\sqrt{x}$, the relatively large temperature difference across the thermal boundary layer leads to significant heating and eventually melting.

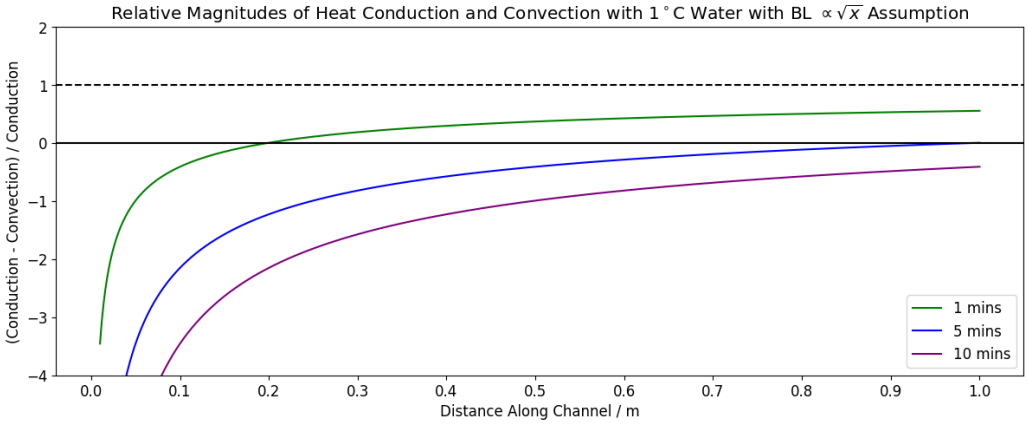

Figure 22: Relative Magnitudes of Conduction and Convection for the $\delta \propto \sqrt{x}$ Assumption

3.5.3 Viscous Shear Channel Flow with a Thermal Boundary Layer

The thermal boundary layer equation for parallel flow is again given by:

$$u\frac{\partial T}{\partial x} = \alpha_{\mathrm{w}}\frac{\partial^2 T}{\partial z^2}$$

Instead of assuming a bulk flow velocity it will be assumed that a velocity boundary layer has developed such that the thermal boundary layer occurs in an area where there is shear flow. The velocity profile will be approximated as $u = Sz$, where S is the shear rate, hence:

$$Sz\frac{\partial T}{\partial x} = \alpha_{\mathrm{w}}\frac{\partial^2 T}{\partial z^2}$$

Taking the same approximations of the temperature differences and thickness δ as above:

$$S\delta\frac{\Delta T_0}{x} \sim \alpha_{\mathrm{w}}\frac{\Delta T_0}{\delta^2}$$

Solving for δ, the thermal boundary layer thickness, now grows with $\sqrt[3]{x}$:

$$\delta \sim \sqrt[3]{\frac{\alpha_{\mathrm{w}} x}{S}}$$

From lubrication theory found in Lister, 1992, the velocity parallel to a slope in a viscous fluid can be described by:

$$u = \frac{g}{2\nu}z(2d - z)\sin\phi$$

When integrated this gives the 2D volumetric flux, V:

$$V = \frac{gd^3}{3\nu}\sin\phi$$

The shear rate is defined as the derivative of velocity with respect to z at the surface:

$$S \equiv \left.\frac{\partial u}{\partial z}\right|_{z=0} = \frac{g\sin\phi}{\nu}d = \left(\frac{g\sin\phi}{\nu}\sqrt{3V}\right)^{2/3}$$

The heat transfer across the new thermal boundary layer can now be derived. Taking the shear velocity profile and once again applying it to the thermal boundary layer equation:

$$Sz\frac{\partial T}{\partial x} = \alpha_{\mathrm{w}}\frac{\partial^2 T}{\partial z^2}$$

Using the similarity solution $T - T_{\mathrm{w0}} = (T_{\mathrm{pc}} - T_{\mathrm{w0}})f(\overline{z})$ where $\overline{z} = z/\delta$ and $\delta = \delta \sim \sqrt{\alpha_{\mathrm{w}} x/S}$ and denoting differentiation with respect to $\overline{z}$ as f':

$$-\frac{1}{3}\overline{z}^2 f' = f''$$

The equation is then separable for f' and can be integrated to give:

$$f' = Ae^{-\overline{z}^3/9}$$

where A is an arbitrary constant. The boundary conditions of phase change temperature at the surface (i.e. $f(0) = 1$) and initial water temperature far from the surface (i.e. $f \to 0$ as $\overline{z} \to \infty$) can be used to integrate f' again to give:

$$f(\overline{z}) = \frac{\int_{\overline{z}}^{\infty} e^{-u^3/9}\, du}{\int_0^{\infty} e^{-u^3/9}\, du}$$

The flux is directly proportional to the temperature gradient at the interface:

$$\left.\frac{\partial T}{\partial z}\right|_{z=0} = \frac{T_f - T_{\mathrm{w0}}}{\delta} f'(0)$$

$$f'(0) = -\left(\int_0^{\infty} e^{-u^3/9}\, du\right)^{-1} \approx -0.538$$

Therefore the heat convection through the ice in the new model of the thermal boundary layer growing with $\sqrt{x}$ is:

$$q_{\mathrm{water}} = 0.548 \lambda_{\mathrm{w}} (T_{\mathrm{w0}} - T_{\mathrm{pc}}) \sqrt[3]{\frac{S}{\alpha_{\mathrm{w}} x}}, \qquad S = \left(\frac{g \sin\phi}{\nu} \sqrt{3V}\right)^{2/3}$$

The above equation interestingly has very little dependence on the flow rate of the water ($q_{\mathrm{water}} \propto V^{1/9}$). The thermal boundary layer also grows much more slowly with distance along the channel, x, than the previous theory, therefore there shall be a slower change in the convection rate. As a result, the ice thickness can be expected to be flatter (as q_{ice} is independent of x). The new equation for the development of the thermal boundary layer can be substituted into the equation for the rate of ice growth which is integrated once more:

$$\rho_{\mathrm{i}} L \frac{\partial \eta}{\partial t} = \frac{\lambda_{\mathrm{i}} (T_{\mathrm{pc}} - T_{\mathrm{i0}})}{\sqrt{\pi \alpha_{\mathrm{i}} t}} - \lambda_{\mathrm{w}} (T_{\mathrm{w0}} - T_{\mathrm{pc}}) \sqrt[3]{\frac{S}{\alpha_{\mathrm{w}} x}}$$

$$\eta(x,t) = \frac{1}{\rho_{\mathrm{i}} L} \left(\frac{2\lambda_{\mathrm{i}} (T_{\mathrm{pc}} - T_{\mathrm{i0}})}{\sqrt{\pi \alpha_{\mathrm{i}}}} \sqrt{t} - \lambda_{\mathrm{w}} (T_{\mathrm{w0}} - T_{\mathrm{pc}}) \sqrt[3]{\frac{S}{\alpha_{\mathrm{w}} x}}\, t \right)$$

The model using a shear flow approximation developed here is an extension to the previous two models by Cartlidge, 2022, as their models bounded the data they obtained. The new model is expected to sit between the two previous models and better capture the shape of the data, as well as fitting to it more accurately.

Figure 23 shows the ice thickness change for the new boundary layer model of a thermal boundary layer in a viscous shear flow. The thermal boundary layer grows more slowly than in the previous case hence, the rate of heat transfer reduces less rapidly. The figure shows an ice thickness thicker than for observed in the previous model (with an inviscid thermal boundary layer) and predict less melting in the channel. Whilst the melting is reduced, there is still melting along the whole length of the channel for 2.0°C water. The melting with 1.0°C water only occurs up to around half the length (~ 0.2 m vs ~ 0.4 m), which is encouraging for the ice volcano if the model is accurate.

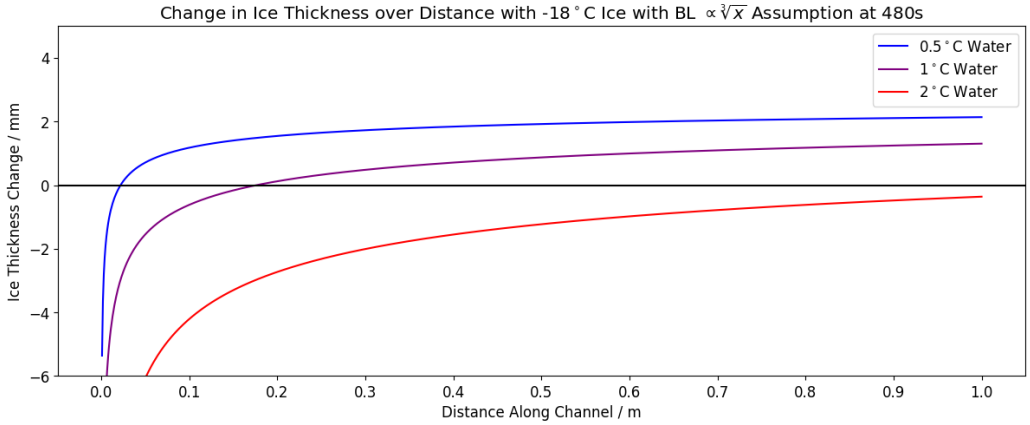

Figure 23: Development of the Ice Profile for the $\delta \propto \sqrt[3]{x}$ Assumption

The impact of the thermal boundary layer growing as the cube root of distance rather than square root as previously is shown in Figure 24. The thermal boundary layer thickens more slowly and hence the rate of convection through it decreases more slowly (with respect to distance). Therefore, the convective heat flux is stronger for further down the channel. The figure shows that after just five minutes there is net heat transfer to the interface (rather than away from it) along most of the channel. Hence, there will be melting along most of the channel.

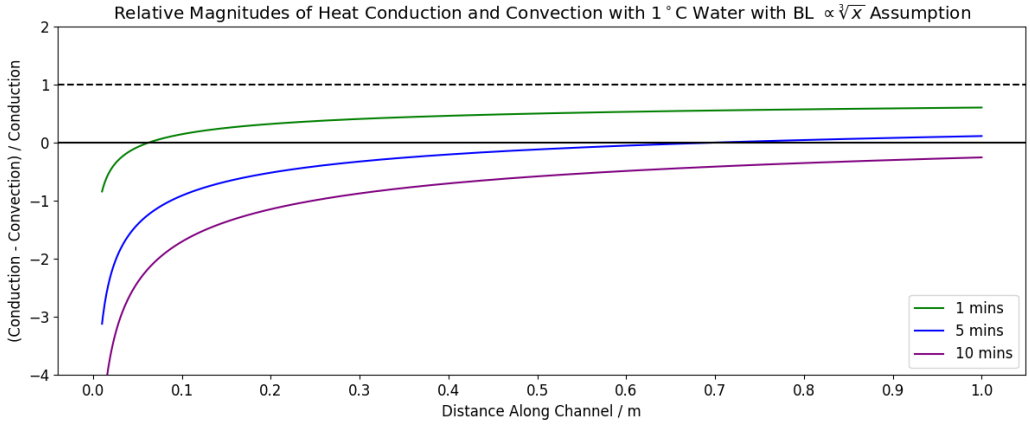

Figure 24: Relative Magnitudes of Conduction and Convection for the $\delta \propto \sqrt[3]{x}$ Assumption

3.5.4 Models for the Development of the Ice Profile - Channel Case

The two models for the ice profile resulting from water flowing over its surface down a channel developed by Cartlidge, 2022 have been supplemented by a third model developed here. The two existing models considered firstly water with a bulk temperature decreasing along the channel due to convection of heat away from the water. The second model considered a thermal boundary layer in a flow of constant (in z) velocity growing with the square root of distance. The new model uses a thermal boundary layer growing within a region of shear flow in a velocity boundary layer; this results in the thermal boundary layer growing as $\sqrt[3]{x}$. All the models show that the heat conduction through the ice initially exceeds the convection to it and hence the first response is freezing. As the ice warms independently of position whilst the heat convection is strongest closest to the channel entry (for all the models), this is where melting first begins (in both space and time). The heat flux by convection is independent of time, hence as the ice warms in time the position of no net flux moves down the channel (in increasing x). The initial water temperature greatly affects the ice profile that develops in all of the models even close to the freezing temperature and with relatively small changes from 0.5°C to 2.0°C, which has significant implications for the ice volcano.

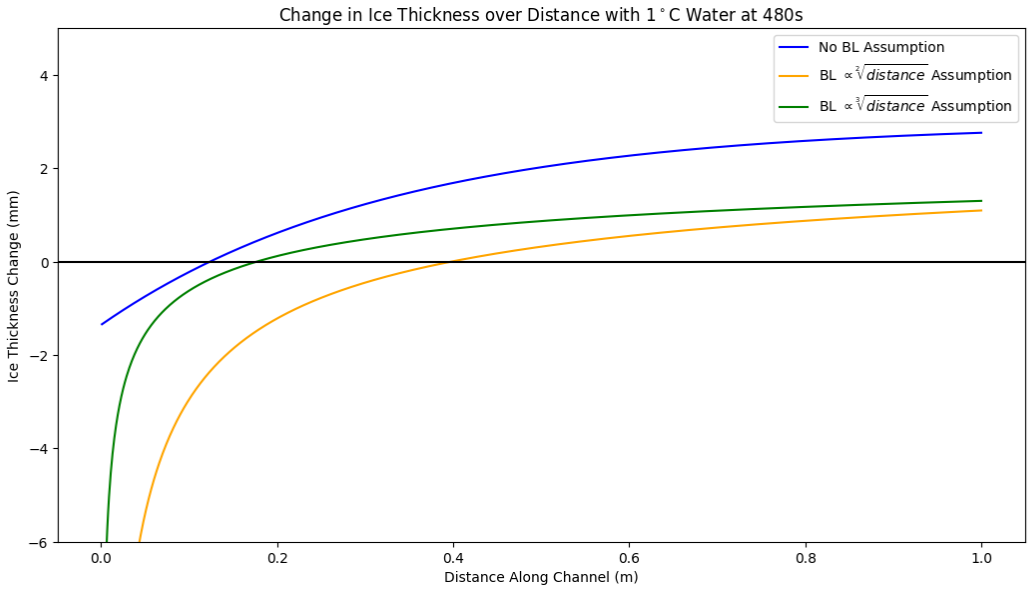

Figure 25: Comparison of the Three Models with 1°C Water after 8 Minutes

Figure 25 shows the prediction of each of the three models for 1°C water flowing over ice down a channel after eight minutes. The new model with a thermal boundary layer in a shear velocity flow predicts a much steeper transition from melting to freezing (at the given time) and sits between the two previous models. Towards the end of the channel the two thermal boundary layer models predict very similar growths, due to the different dependencies on distance along the channel. These models cross at $x \approx 2\,\mathrm{m}$ though this is outside the range of interest of this project which focuses on relatively short length scales.

4 Experiments - Channel Flow

4.1 Experimental Setup - Channel Flow

Cartlidge, 2022 conducted experiments in a walk-in meat freezer in the kitchens of Trinity College, Cambridge to determine the ice profile resulting from water flowing over its surface and down a channel. The freezer was used as a cold room, maintained at -18°C, representative of Arctic temperatures in the winter (Labe, 2016). The same experimental setup (shown in Figure 26) involved pumping water from a reservoir to the inlet of a slightly angled channel and then into a collection container. This was used in the following experiments.

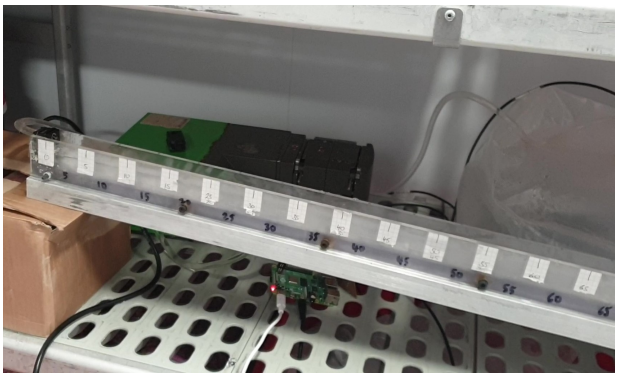

Figure 26: Channel Setup

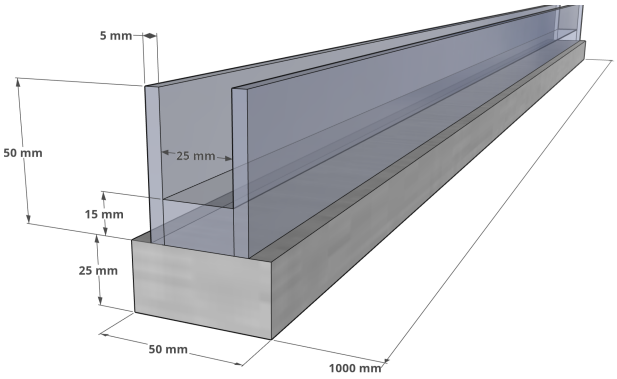

Figure 27: Channel Size (Cartlidge, 2022)

The pump used was calibrated to a volumetric flow rate of water of $5.4\,\mathrm{cm^3 s^{-1}}$ and the channel (shown in Figure 27), had an aluminium base to act as a heat sink with an acrylic channel on top. Acrylic was used for two reasons; first its transparency allows the basic ice profile to be seen through the walls. Secondly, any heat transfer to the walls is neglected in the models, hence the low thermal conductivity of acrylic helped to minimise heat transfer from the water/ice and the walls. The walls did however, provide a challenge in achieving a uniform ice profile across the width of the channel as discussed later.

The channel was designed such that its entire width was uniformly covered by a thin film of water at the selected flow rate, hence the model could be assumed to be valid over the whole width and uniform growth was expected. The characteristic distance of the temperature signal, $l \backsim \sqrt{\alpha_\mathrm{i} t}$, is approximately 24 mm after eight minutes. The depth of ice frozen was slightly shallower than this hence the semi-infinite approximation may start to break down towards the end of the 8 minute experiment. Before the temperature signal reaches the base of the ice it is unaware that the ice is not semi-infinite and hence the assumption is valid until this point. Originally the channel was taped closed, however it was very challenging to prevent water from leaking. Therefore, two stoppers which were 3D-printed by Pantling, 2022, these have slots for o-rings to sit into and are then sealed with a non-hardening sealant to prevent water escaping. Initially, the ice does not freeze evenly so it is melted using a warmed strip of aluminium (similar to a *Zamboni* for ice-rinks, Cartlidge, 2022), before being allowed to refreeze. The process of melting and refreezing must often be carried out multiple times to ensure that the surface of the ice is suitably smooth to carry out the experiment.

The change in ice thickness was measured as the difference between two measurements from the top of the channel. Before running water over the surface a micrometer was used to measure the depth from the top of the channel at two locations across its width at 5 cm intervals. After the experiment the ice was allowed to cool (to prevent the micrometer melting the ice) and measurements were taken at the same locations and the difference between their averages taken as the change in the ice profile. Due to natural variations across the width of the channel this measurement incurred significant uncertainty, hence two measurements were taken across the channel width.

4.2 Achieving Freezing Temperature Water

Cartlidge, 2022 performed experiments using freezing temperature water flowing down ice over the channel, however it was noted there was significant difficulty in maintaining the temperature of the water. By melting ice cubes into water it is possible to cool the water to 0°C in the reservoir and this is known to be constant if further ice cubes do not melt. However, as noted above, there is some cooling in the water pipe that leads to a temperature drop (for above freezing temperature water). In the case of water at or close to freezing temperature (<1°C) it is observed that the water begins to freeze in the supply pipe as shown in Figures 28 and 29. Maintaining a constant supply of water with no ice was not practical with the available equipment and on the rare occasion ice did not block the pipe, particles of ice were observed in the flow. In the experiments of Cartlidge, 2022, greater than expected ice buildup was observed for freezing temperature water, possibly as a result of some freezing occurring before the water reaches the channel. As a result of the difficulty pumping water at its freezing temperature it was decided that it would be futile to continue with experiments at freezing temperature. These may be possible with more direct control of the heat transfer to/from the water however this was not possible in this project.

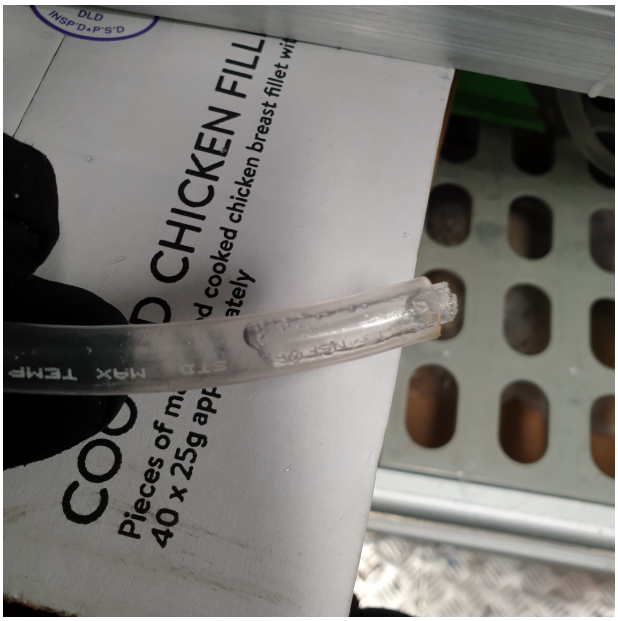

Figure 28: Freezing in the Pipe

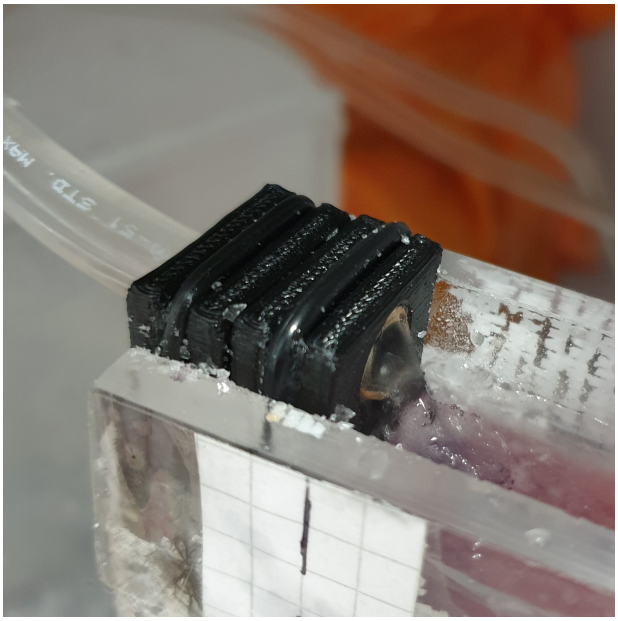

Figure 29: Freezing at the Inlet

4.3 Raspberry Pi Thermocouples for Temperature Measurement

When Pantling, 2022 repeated the experiments of Cartlidge, 2022 it was identified that the results were not reliable. It was suggested that inaccurate knowledge of the water temperature could be the cause due to the large differences in ice profile observed with small changes to the water inlet temperature in the models. In those experiments the water temperature was assumed to be the temperature of the fridge where the water was stored (2°C) before being taken out briefly for experiments. However, 1°C temperature variations may have occurred in the fridge which is constantly opened for placing/removing food. Therefore, in this project thermocouples were set up connected to a Raspberry Pi (RPi) to measure the water temperature. Initially, the thermocouples shown in Figure 30 were soldered to a breadboard and connected to the RPi. Code was then written on the RPi to receive temperatures from all thermocouples every second, this was either to record temperatures throughout the length of the experiment or to display them for an indefinite period. The RPi was connected to a smartphone through ssh using the *RaspController* app, which allowed the RPi to be controlled remotely without the need for a wired keyboard, mouse or display. SSH allows two computers to securely communicate over a network and can be used through the mobile hotspot of a smartphone. The thermocouples acquired at first, when tested, were too large to measure the temperature of the relatively small film of water flowing over the surface of the ice, hence they were measuring the temperature of the surrounding air. Smaller, identical, thermocouples were then acquired with no pre-waterproofing, these were then waterproofed by potting them into a shrink-fit and wired to a new breadboard. These thermocouples (shown in Figure 31) respond much more quickly to temperature changes, however, they are still too large to measure the temperature of the water flowing over the ice. Therefore, an experiment was performed with water flowing from the reservoir through the pump and back in whilst the inlet and outlet temperatures were measured. The temperatures were measured continuously whilst the reservoir water temperature dropped and the temperature difference across a range of temperatures was approximately 1.0°C. In the following experiments designed to imitate the ice volcano the reservoir temperature was measured and this was set to be 1.0°C warmer than the desired inlet temperature.

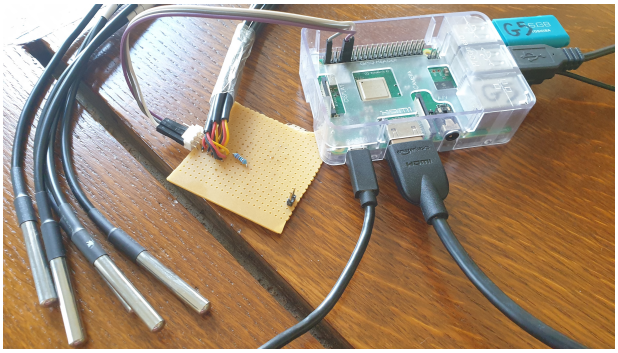

Figure 30: Original Thermocouples

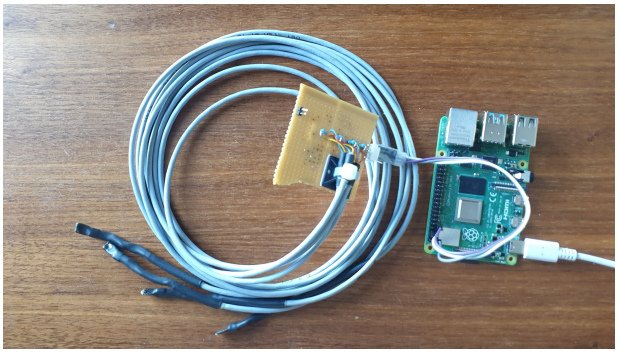

Figure 31: New, Smaller Thermocouples

5 Results and Discussion - Channel Flow

Experiments were performed for water entering the channel at 2.0, 0.8 and 0.5°C. The water flowed over the ice surface for eight minutes in each experiment before any excess was poured off and the new profile measured. The change in ice thickness was measured at nineteen 5 cm intervals down the length of the channel. These measurements are plotted with the three models evaluated at the water temperature. The error bars on the plots are ±0.5 mm due to the variation of the ice thickness across the channel width. In all experiments there was often melting at the channel inlet that was beyond the measuring range of the micrometer (10 – 15 mm depending on the initial ice depth). The no thermal boundary layer model predicts freezing/very little melting which is not observed. Meanwhile, infinite melting is predicted at $x = 0$ by both thermal boundary layer models for $t > 0$ as a result of the thermal boundary layer breaking down there. The ice melting at the inlet was also affected by the water not immediately forming a thin film when exiting the pipe, hence the validity of these points is disputable both for the models and measurements.

5.1 Results for 0.5°C Water

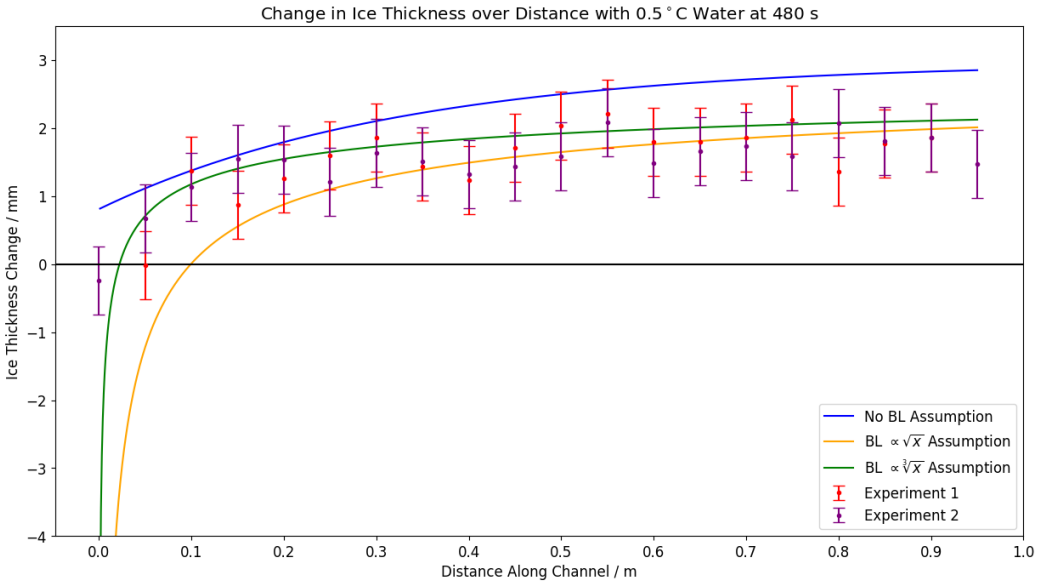

Figure 32: Experimental Results for 0.5°C Inlet Water

Figure 32 shows the measured and predicted ice profiles for water entering the channel at 0.5°C, the two data sets show that the experiment is reliable when the inlet temperature is measured. Each data point is the average of two measurements taken across the width of the channel in each experiment. The experimental data fits to the new model ($\delta \propto \sqrt[3]{x}$) better than the previous models as was expected as this model is between the previous two. Towards the end of the channel the new model slightly overestimates the amount of freezing that shall occur and the previous boundary layer model ($\delta \propto \sqrt{x}$) is slightly more accurate.

5.2 Results for 0.8°C Water

The 0.8°C experiment showed more melting close to the channel inlet and less freezing than the previous experiment as predicted both intuitively and by the models (Figure 33). After the same time of eight minutes, more melting was observed close to the channel inlet and there was slightly less freezing further down the channel. The two sets of experimental results are very similar although there are a few outliers in the results of *Experiment 1* (at $x = 0.35$ and $x = 0.95$ in particular). The data matches with the newly developed viscous thermal boundary layer theory ($\delta \propto \sqrt[3]{x}$) all the way along the channel where previously it overestimated the growth. Once again the no thermal boundary layer approximation fails to capture the observed ice melting very close to the channel inlet and predicts around twice the average observed water freezing at the end of the channel. There is a small region around 0.2 m from the inlet where the no thermal boundary layer model provides a reasonable estimate of the growth, however this is very small. The results for both water temperatures suggest that there is a thermal boundary layer in the water and that it is not well mixed. After the water reaches the halfway point of the channel the two thermal boundary layer models are almost equivalent with the new model slightly more accurate.

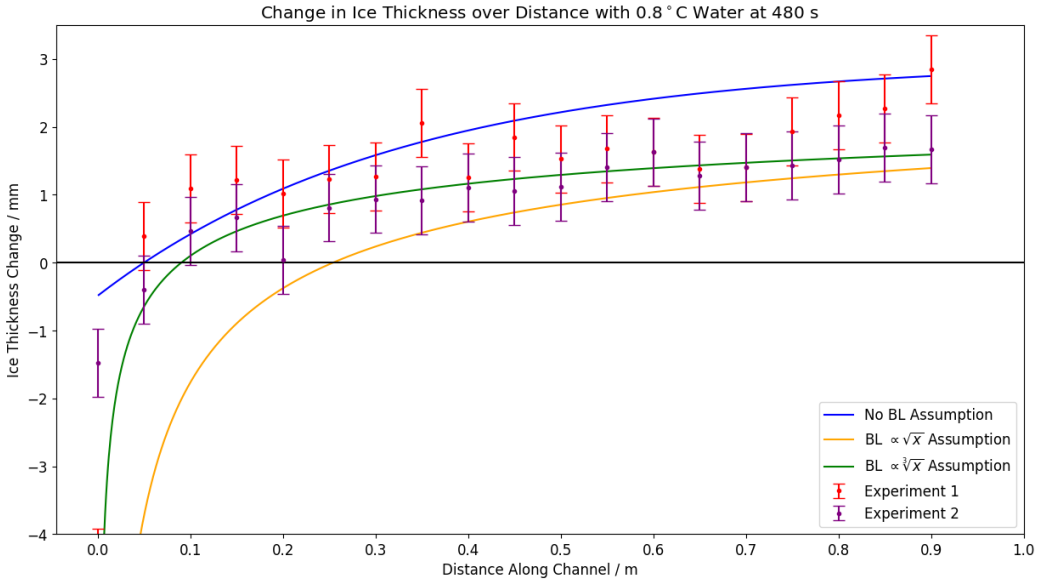

Figure 33: Experimental Results for 0.8°C Inlet Water

5.3 Results for 2.0°C Water

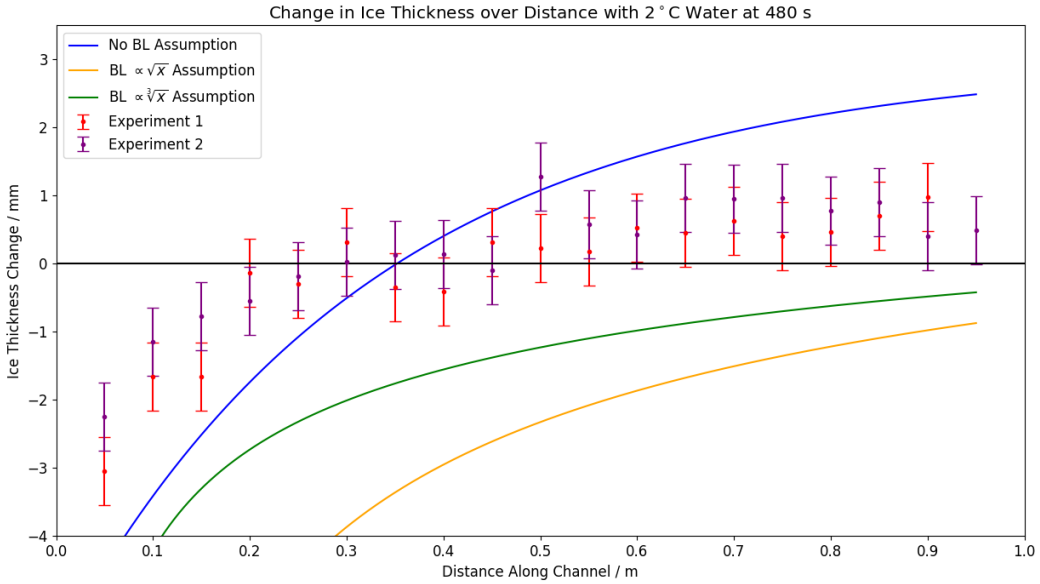

Figure 34: Experimental Results for 2.0°C Inlet Water

The results for water at 2.0°C entering the channel do not fit the models as the two colder experiments did. The melting close to the channel inlet is vastly over predicted by all the models, including the no thermal boundary layer model. Meanwhile, melting is predicted by both of the thermal boundary layer models at the end of the channel where freezing is observed, the no thermal boundary layer model does not accurately describe the freezing either. There are a few possible reasons for the inaccuracy of the model with 2.0°C water. Firstly the severe melting observed (and predicted) before net freezing after eight minutes causes multiple assumptions to perhaps be invalidated. The models for the heat transfer assume that there is a thin film of water flowing over the surface of the ice, with the melting observed (which was all the way through the ice at $x = 0$ and hence not plotted), the water sits in the hole which it has created and does not flow. The models also neglect the effects of the moving interface in heat transfer; for the colder temperatures the melting was relatively small (order 1 mm) after a short distance, whereas for 2.0°C water the melting is greater and lasts further down the channel. Hence, this assumption is less valid for more of the channel and could explain the discrepancy. There is a small possibility that the water was colder than the 2.0°C expected from the exit of the pipe. The minimum root mean square error for the average of the 2.0°C data is at 1.2°C where the data fits the $\delta \propto \sqrt[3]{x}$ model accurately. It is however unlikely that the temperature measurement would be incorrect in both experiments and as the two data sets are consistent, a systematic error or breakdown of the model provides a better explanation of why the models do not accurately predict the ice growth.

5.4 Additional Observations - Channel Flow

The ice profile along the length of the channel was often highly irregular across the width of the channel: the most frequent irregularity was ice growth along one side of the channel rather than the other along a section before the same was observed on the opposite side. The formations are reminiscent of sandy banks intruding into river bends and are shown in Figures 35 and 36.

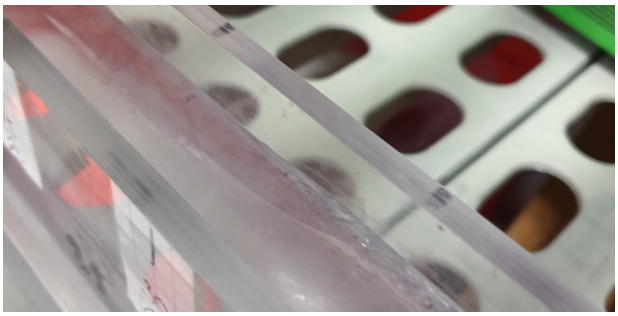

Figure 35: Side Growth Image 1

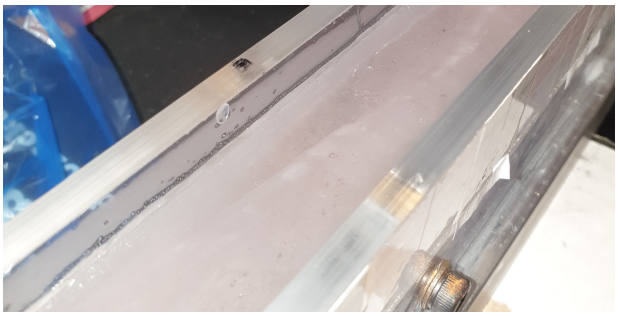

Figure 36: Side Growth Image 2

Figure 37 shows a basic diagram of the ice formation with the lower and upper surfaces having a height difference of the order of 1 mm, similar to the measured water freezing in successful experiments. The variation across the width of the channel is thought to be due to the walls, these are made of acrylic so there should be very little heat transfer. However, they may have provided nucleation points for ice to grow preferentially; the curved shape of the growths implies this may have been the case.

Figure 37: Side Growth Diagram

Figure 38: Ice Ridge

There was one case in which a ridge developed, weaving along the middle of the channel as shown in Figure 38. There was a distinctive peak in the ice along almost the whole length where freezing was expected with a difference of between 1 and 2 mm in height across the channel. This formation cannot be explained by nucleation on the channel walls and it is not known why it occurred; during many experiments the formation appeared only once.

6 Modelling - Radial Flow

6.1 Setting Up the New Problem

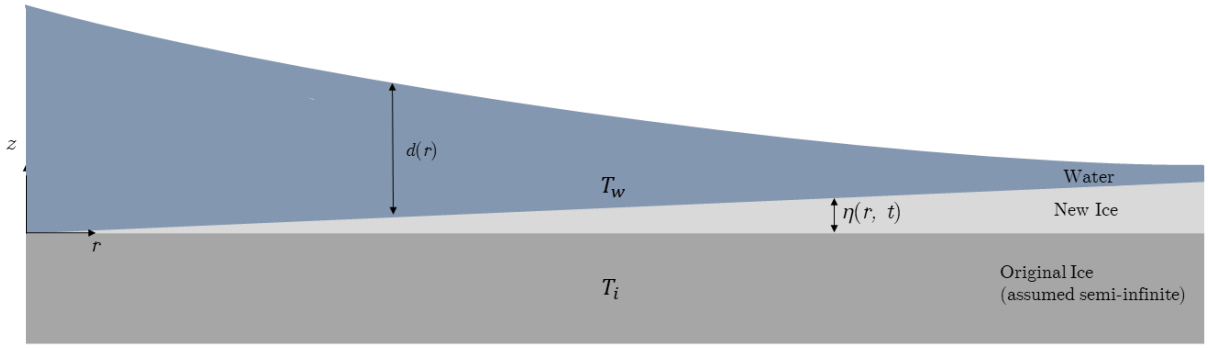

Figure 39: Theoretical Model of Water Radially Over Semi-Infinite Ice

The development of the ice profile in three dimensions is more complex with the setup for solving the problem shown in Figure 49. The water now flows radially outwards from the origin and is assumed to be axisymmetric. At $r = 0$ the water has temperature T_{w0} and velocity v with some depth d. The mass flow rate is constant (as freezing/melting is negligible), as is the density, therefore dvr is constant where r is the radial position. A streamline on the surface of the water can now be considered with the gravitational term neglected: $p_0 = p + {}^1\!/\!_2 \rho_w v^2$. The pressure at all locations is atmospheric (so constant) hence the surface velocity, v, is also constant. Therefore the depth is inversely proportional to the radial position (i.e. $d \propto 1/r$). Once again the change in ice thickness, η, may be either positive or negative depending on the balance of conduction and radiation. The ice is still assumed to be semi-infinite such that the temperature signal does not fully penetrate the ice during the experiment. The flow is only considered in the region in which a thin film covers the surface of the ice before any rivulets have formed (which would be of importance in the ice volcano). These assumptions greatly simplify the true conditions of the ice volcano that would operate on ice that is not level, has surface deformations and is not semi-infinite, however it provides a better representation of the true flow than the channel model. Considering the model for the channel case it is difficult to intuitively predict what may happen with the radial flow. As the water flows outwards its mass flow rate per unit area will reduce and hence we expect the convective heat flux to reduce similarly. Meanwhile, the conductive heat flux was independent of position for the channel. Therefore, it may be found that there is a position after which only freezing can occur (for a specific temperature). The origin will be provided with a constant flux of heat from the supply of hot water and so melting is expected at the centre of the ice. However, it is difficult to instinctively predict how the melting will expand outwards and where the limit of melting may be, if there is one.

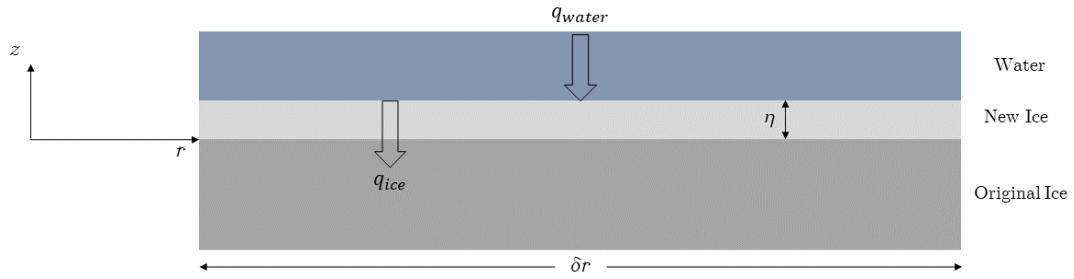

Figure 40: Heat Transfers in the Radial System

The heat flux by conduction through the ice is identical to the channel case and is directly proportional to the local temperature gradient at the surface. As before this will be approximated as at the initial interface $z = 0$:

$$q_{\text{ice}}(r,t) \propto \left.\frac{\partial T_{\text{i}}}{\partial z}\right|_{z=0} = \lambda_{\text{i}} \left.\frac{\partial T_{\text{i}}}{\partial z}\right|_{z=0}$$

Where the symbols have the same meanings as defined previously though T_{i} shall now potentially vary in r rather than in x.

The heat flux to the interface from the water can also be described like previously as proportional to the temperature difference between the water and the interface:

$$q_{\text{water}}(r,t) \propto (T_{\text{w}} - T_{\text{interface}}) = h(T_{\text{w}} - T_{\text{pc}})$$

where T_{w} is the temperature of the water at any position in space (r or z) and time.

The conditions at the interface shall remain identical to those in the channel case; the temperature of both the ice and water at the interface must be equal to the phase change temperature for all time at any radial position:

$$T_{\text{i}}(r,0,t) = T_{\text{w}}(r,0,t) = T_{\text{pc}}$$

Also the conditions as to the initial behaviour are identical; at the instant the water makes contact with the ice there must be an infinite temperature gradient in the ice. Its surface must be at the phase change temperature and just below the surface it must be at the initial temperature, i.e. $T_{\text{i}}(r,0,0^+) = T_{\text{pc}}$ and $T_{\text{i}}(r,0^-,0^+) = T_{\text{i0}}$. Therefore, in the case of a radial flow the first response of the system must be freezing of the water at an infinite rate, independent of the initial temperature of the water.

$$\left.\frac{\partial T_{\text{i}}}{\partial z}\right|_{z=0} \to \infty \;:\qquad q_{\text{ice}} \to \infty \;:\qquad \frac{\partial \eta}{\partial t} \to \infty \qquad (t = 0^+)$$

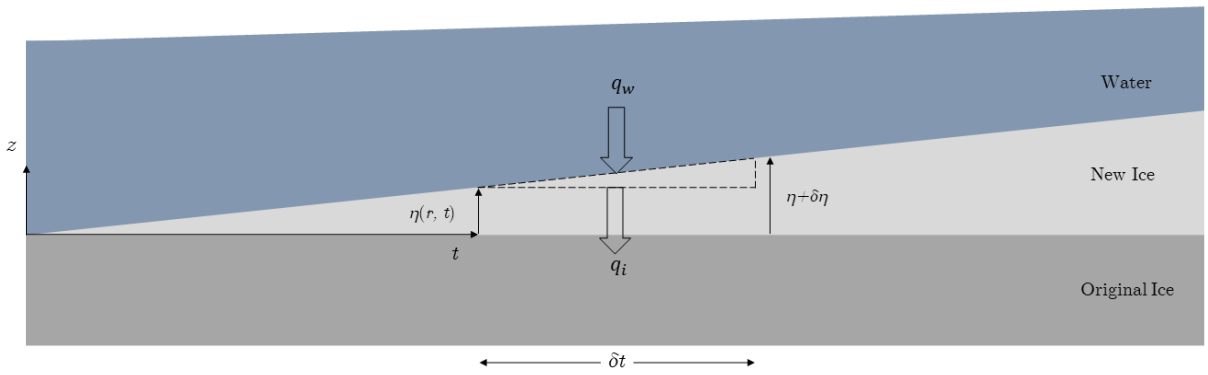

Figure 41: Control Volume at the Interface for the Radial Case

Taking a per unit area analysis over a time period δt, a heat balance can be applied to find the rate of ice growth for the case of the radial flow. As each of the fluxes of heat (conduction, convection and latent) is identical to the channel case the equation is identical, though η is now a function of radial position rather than distance down the channel as previously. The equation for the rate of ice growth ignoring the moving interface is:

$$\rho_{\mathrm{i}} L \frac{\partial \eta}{\partial t} = \lambda_{\mathrm{i}} \left. \frac{\partial T_{\mathrm{i}}}{\partial z} \right|_{z=0} - h(T_{\mathrm{w}} - T_{\mathrm{pc}})$$

6.2 Radial Heat Conduction Through the Ice

The temperature profile in the ice can be derived for the radial case using the heat diffusion equation. The radial velocity of the water shall be considered to be much greater than the characteristic velocity of the temperature signal in the ice and hence the temperature can be assumed to be independent of radius:

$$\frac{\partial T_{\mathrm{i}}}{\partial t} = \alpha_{\mathrm{i}} \nabla^2 T_{\mathrm{i}} = \alpha_{\mathrm{i}} \frac{\partial^2 T_{\mathrm{i}}}{\partial z^2}$$

The solution to this equation is given below, as the boundary conditions are also identical to the channel case the same solution for the ice temperature is obtained:

$$T_{\mathrm{i}}(z,t) = T_{\mathrm{pc}} + (T_{\mathrm{pc}} - T_{\mathrm{i0}}) \operatorname{erf}\left(\frac{z}{2\sqrt{\alpha_{\mathrm{i}} t}}\right)$$

This result is interesting, if expected, as it shows that the ice response is unaffected by the conditions of the water on the surface. The heat conducted through the ice follows from the ice profile and is therefore independent of the radial position:

$$q_{\mathrm{ice}} = \frac{\lambda_{\mathrm{i}}(T_{\mathrm{pc}} - T_{\mathrm{i0}})}{\sqrt{\pi \alpha_{\mathrm{i}} t}}$$

6.3 Inviscid Radial Flow with No Thermal Boundary Layer

The first assumption made for the heat convection from the water is that it is well mixed at some bulk temperature which decreases as the flow spreads radially outwards. The temperature is expected to decrease at a much faster rate than in the channel case as the heat capacity of the water per unit area shall decrease with radius. The heat transfer from the control volume shown in Figure 42, q_{water} is $h(T_{\text{w}} - T_{\text{pc}})$ where T_{w} is the temperature of the water at position r and time t.

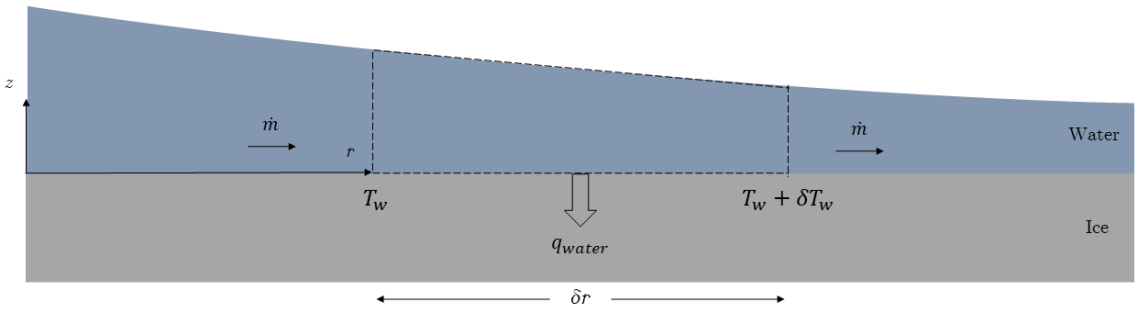

Figure 42: Control Volume for Deriving the Radial Water Temperature Profile

The control volume in Figure 42 represents an asymmetric annulus at r of width δr. Applying energy conservation to this control volume:

$$\dot{m}c_{\text{p,w}}(T_{\text{w}} + \delta T_{\text{w}}) - \dot{m}c_{\text{p,w}}T_{\text{w}} = -q_{\text{water}} \cdot 2\pi r \delta r$$

$$\dot{m}c_{\text{p,w}}\delta T_{\text{w}} = -h(T_{\text{w}} - T_{\text{pc}}) \cdot 2\pi r \delta r$$

The phase change temperature is a constant, hence $\delta T_{\text{pc}} = 0$, $\delta(T_{\text{w}} - T_{\text{pc}}) \equiv \delta T_{\text{w}}$ and:

$$\frac{\delta(T_{\text{w}} - T_f)}{T_{\text{w}} - T_f} = -\frac{2\pi h}{\dot{m}c_{p,w}} r \delta r$$

The above equation can be integrated from T_{w0} at $r = 0$ to T_{w} at r to give an equation for the cooling of the water as it flows outwards:

$$\int_{T_{\text{w0}}}^{T_{\text{w}}} \frac{1}{T_{\text{w}} - T_f} d(T_{\text{w}} - T_f) = -\frac{2\pi h}{\dot{m}c_{p,w}} \int_0^r r\, dr$$

$$\left[\ln\left(T_{w,r} - T_f\right)\right]_{T_{\text{w0}}}^{T_{\text{w}}} = -\frac{2\pi h}{\dot{m}c_{p,w}} \left[r^2/2\right]_0^r$$

$$\ln\left(\frac{T_{\text{w}} - T_f}{T_{\text{w0}} - T_f}\right) = -\frac{\pi h}{\dot{m}c_{p,w}} r^2$$

$$T_{\text{w}} = T_f + (T_{\text{w0}} - T_f) \exp\left(-\frac{\pi h}{\dot{m}c_{p,w}} r^2\right)$$

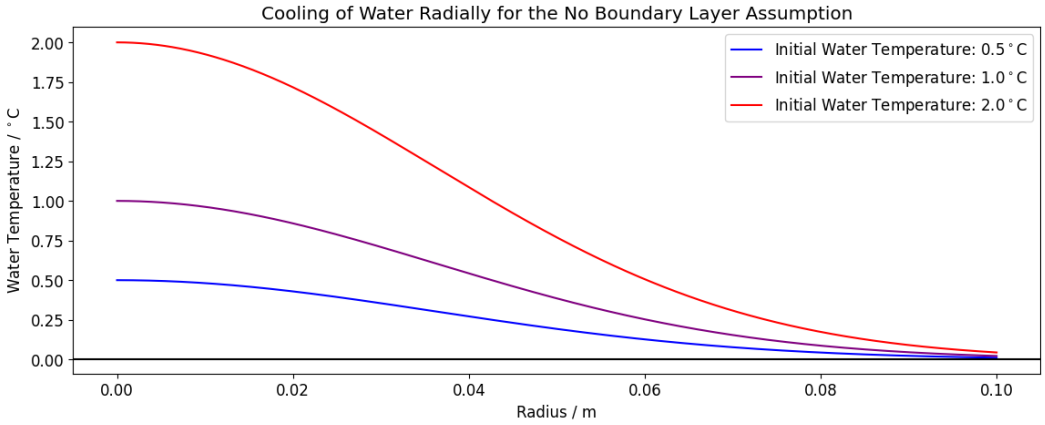

Figure 43: Water Temperatures Radially

The water temperature decreases to close to the phase change temperature much more rapidly for the radial case as expected. The temperature decreases exponentially with the square of radius, $\Delta T \propto \Delta T_0 \exp(r^2)$, in contrast to the purely exponential decrease seen in the case of the channel flow $\Delta T \propto \Delta T_0 \exp(x)$. The difference in the rate at which the temperature approaches phase change temperature is stark with the radial temperature reaching close to zero after just 0.1 m, as shown in Figure 43, compared with the almost metre required for the channel (Figure 18). The rapid temperature reduction implies that there may be ice growth closer to the origin even after longer periods of time.

The equation for the radial cooling of water flowing over ice can be substituted into the equation for the rate of ice thickness change giving:

$$\rho_\mathrm{i} L \frac{\partial n}{\partial t} = \frac{\lambda_\mathrm{i}(T_f - T_{\mathrm{i}0})}{\sqrt{\alpha_\mathrm{i}\pi t}} - h(T_{\mathrm{w}0} - T_f)\exp\left(-\frac{\pi h}{\dot{m} c_{p,w}} r^2\right)$$

Integrating the equation to find the resulting ice profile is trivial:

$$\eta = \frac{1}{\rho_\mathrm{i} L}\left(\frac{2\lambda_\mathrm{i}(T_f - T_{\mathrm{i}0})}{\sqrt{\alpha_\mathrm{i}\pi}}\sqrt{t} - h(T_{\mathrm{w}0} - T_f)e^{-\frac{\pi h}{\dot{m} c_{p,w}} r^2}\, t\right)$$

As shown in the equation above, the ice profile resulting from radial flow with no thermal boundary layer will quickly tend to grow (in space) for any time as the convective term will quickly become negligible. The general form of the equation is very similar to the channel case so a similar shape of the profile is expected, though this will be over a smaller distance. The equation again predicts that there will be melting in the centre after a period of time; this is highly undesirable for the ice volcano. If melting in the centre of the ice volcano cannot be avoided then it will quickly become useless. However, it is important to note that the model predicts melting in the centre and growth further outwards, which may result in a bowl shape that can be intermittently left full of water to freeze. Methods for mitigating the melting effect are discussed later.

The ice profiles after five minutes for three different temperatures are shown in Figure 44. There is melting in the centre where the water is warmest and convection is strongest then freezing where the water has cooled. The ice profile is clearly symmetric (with the only r term being squared in the exponential), however, it is useful to visualise a full slice across the diameter of a disk. The ice profile differs significantly from that in the channel case (Figure 19) as the profile appears more co-sinusoidal at the origin leading to a smooth transition from the origin. The channel model, if reflected in the x-axis would have a discontinuous slope at the origin. As the water temperature reduces so rapidly, constant ice growth of $\sim 2.4\,\text{mm}$ after 5 minutes is achieved at a radius of approximately 0.1m.

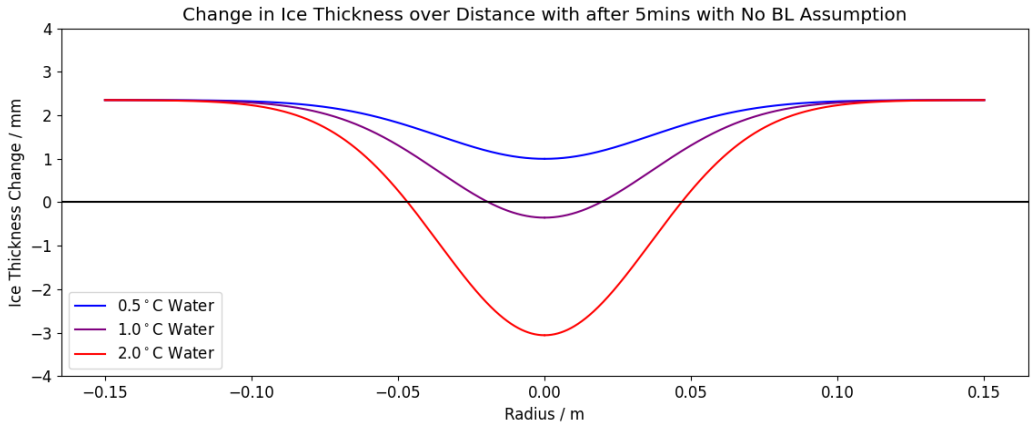

Figure 44: Development of the Radial Ice Profile with the No Thermal Boundary Layer Assumption

The relative magnitudes of conduction and convection are plotted in Figure 45 showing how the conduction quickly exceeds the convection (the dotted line in the figure). The point at which the plots cross the axis is the point at which there is a change from instantaneous growth (above the axis) to instantaneous freezing (below the axis). Once melting begins to occur there is no mechanism to prevent it, so the ice only shall continue to melt.

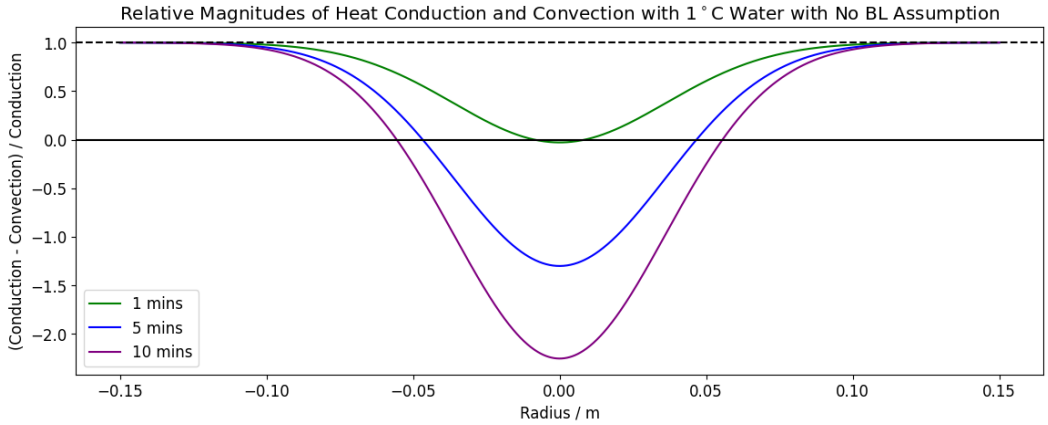

Figure 45: Relative Magnitudes of Conduction and Convection for the NBL Assumption

6.4 Inviscid Radial Flow with a Thermal Boundary Layer

The thermal boundary layer equation for parallel flow radially from a source is:

$$u\frac{\partial T}{\partial r} = \alpha_{\mathrm{w}}\frac{\partial^2 T}{\partial z^2}$$

The first approximation that shall be made is the same as for the first boundary model layer for the channel; a bulk velocity, v, that is constant above the interface. Taking the initial temperature difference between the water and the interface to be ΔT_0 and the thermal boundary layer thickness to be δ:

$$v\frac{\Delta T_0}{r} \sim \alpha_{\mathrm{w}}\frac{\Delta T_0}{\delta^2}$$

The thermal boundary layer thickness can then be solved for and shown to grow with $\sqrt{r}$:

$$\delta \sim \sqrt{\frac{\alpha_{\mathrm{w}} r}{v}}$$

Hence the thermal boundary layer grows equally quickly in the radial and channel cases, which is perhaps intuitive as the thermal boundary layer grows in the region close to the surface (and therefore is unaffected by the water depth). As the water spreads more enthalpy is drawn in from above the thermal boundary layer but this is balanced by the increase in convective cooling and as a result the thermal boundary layer depth grows as before.

Using the above equation in the model for ice growth gives the following result:

$$\eta(r,t) = \frac{1}{\rho_{\mathrm{i}} L}\left(\frac{2\lambda_{\mathrm{i}}(T_{\mathrm{pc}} - T_{\mathrm{i0}})}{\sqrt{\pi\alpha_{\mathrm{i}}}}\sqrt{t} - \lambda_{\mathrm{w}}(T_{\mathrm{w0}} - T_{\mathrm{pc}})\sqrt{\frac{v}{\alpha_{\mathrm{w}} r}}\, t\right)$$

Hence the ice profile is equivalent to the channel case for the thermal boundary layer growing in a flow with a constant, bulk, velocity. The ice profile is shown in Figure 46, the model melting at the centre of the ice but the convection quickly reduces such that there is net freezing after five minutes with both 0.5 and 1.0°C water.

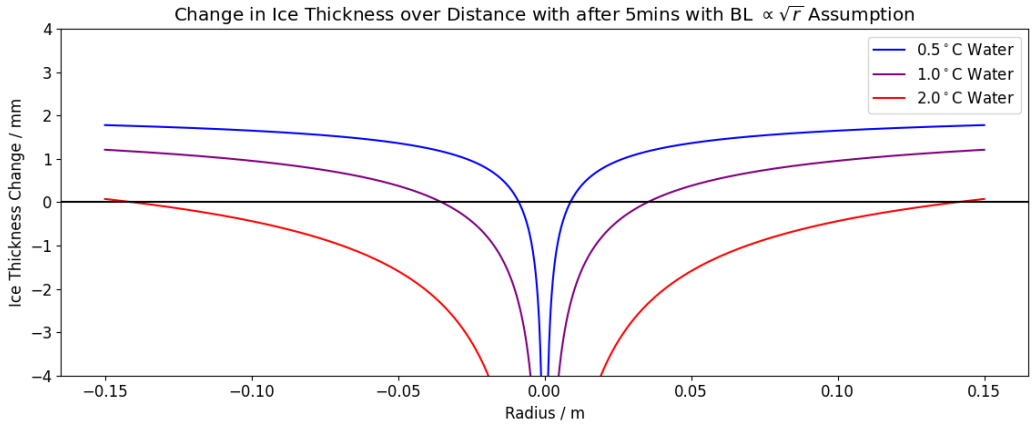

Figure 46: Development of the Radial Ice Profile for the $\delta \propto \sqrt{r}$ Assumption

6.5 Water with a Thermal Boundary Layer Growing in Shear Flow

For the case of water flowing down a channel the heat transfer over a thermal boundary layer in a shear velocity flow was calculated. The velocity profile was taken to be increasing linearly with distance from the surface ($u = Sz$) up to the surface at a constant depth, d. In the radial case the flow spreads out with only mass flow rate constant, hence as the flow spreads out udr is constant. For the above models the flow is assumed to be inviscid, hence u is also constant and $d \propto 1/r$. However, in a shear velocity flow, u is not constant with respect to r and hence the thermal boundary layer thickness is non-trivial to derive. Deriving the thermal boundary layer for a shear velocity flow spreading radially from a source would provide a third model to be used for predicting the ice profile but was not possible in this project due to time constraints.

6.6 Models for the Development of the Ice Profile - Radial Case

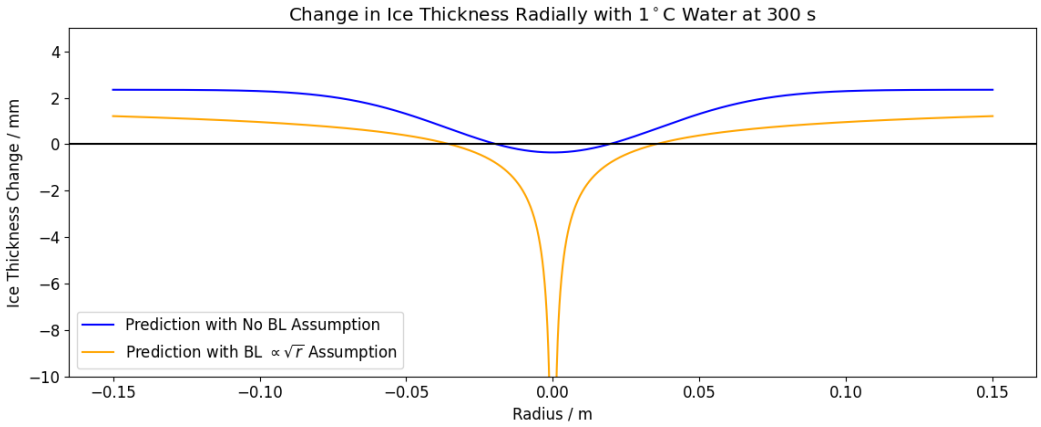

Figure 47: Comparison of the Models with 1°C Water after 5 Minutes

The models predicting the development of the ice profile for the radial flow are shown in Figure 47. There is once again severe melting predicted by the thermal boundary layer model and a small amount of melting predicted by the no thermal boundary layer model. The ice thickness after 0.1 m is expected to reach $1 - 3$ mm after water has flowed over the surface for five minutes with 1°C water. For the channel flow the data was between the no thermal boundary layer and $\delta \propto \sqrt{x}$ models; if this is again the case then melting is expected up to ~ 0.25 m after which there may be freezing. The melting is predicted by the thermal boundary layer model to be most severe in a ~ 10 mm diameter region around the origin with a smooth transition to freezing as observed in the channel case.

7 Experimental Setup - Radial Flow

The challenges presented by working in the walk-in meat freezer of the Trinity College kitchens led to the procurement of a chest freezer to be used for the radial experiments. The new freezer could be accessed at any time of the day and presented a significantly reduced risk of frostbite or hypothermia as only the experiment rig was inside the cold environment. The more rapid reduction in water temperature due to radial spreading allowed for a smaller experimental rig to be designed for the radial flow. The rig shown in Figure 48 was developed to hold a disc of ice and measure the profile with the attached digital micrometer. The same pump as used before (with the same flow rate) was used to pump water through the pipe shown onto the centre of the ice surface. The ice disk was frozen in a flexible silicone cake tin on top of a thin solid aluminium disk so that it could be easily removed. The method did not provide a smooth surface of ice with the thickness varying by over 5 mm, so repeated melting and refreezing was required. Also, a challenge in obtaining a suitable ice disk was air pockets forming near the surface. This may due to the ice freezing on the surface first then air being trapped underneath and forming the air pockets. It is recommended that an ice disk is frozen vertically, constrained on the two flat surfaces for any future experiments.

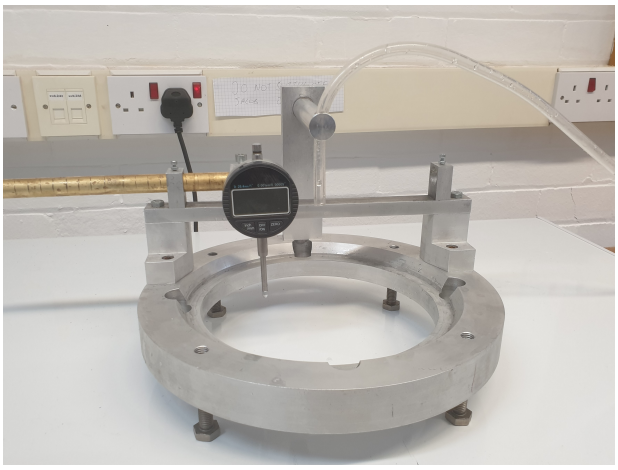

Figure 48: Radial Flow Rig

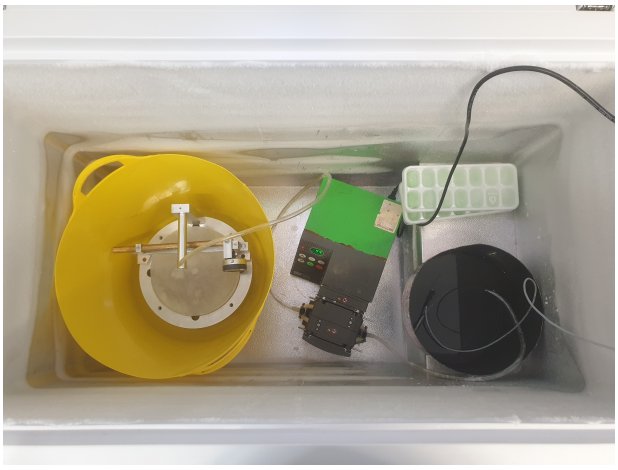

Figure 49: Radial Flow Setup

As a result of the smaller size of the setup, an experiment time of 5 minutes was selected for the radial experiments with the intention of measuring both melting and freezing. The ice was frozen to a similar thickness hence the semi-infinite assumption remains valid for the radial experiments. Once the ice was placed into the rig it was placed into the freezer and allowed to cool to prevent the micrometer melting the ice upon measurement. Before and after the experiment, the micrometer was used to measure at 10 mm intervals across a diameter of the ice disk and the difference taken to be the change in ice thickness. The design of the rig and the ice freezing onto it did not permit measurements across multiple diameters, however, with a design that permitted movement of the micrometer this could be achieved. The temperature drop of water through the pipe in the chest freezer was measured as before and found to be the same as that in the walk-in freezer. Therefore, the measured water reservoir temperature was set again to be 1.0°C warmer than the desired exit temperature from the pipe onto the ice.

8 Results and Discussion - Radial Flow

8.1 Experiments with 1.0°C Water

Two experiments were carried out with 1°C water flowing over the ice disk for five minutes. At 10 mm intervals from the centre of the ice disk the change in ice thickness was measured and the data plotted against the radial models as shown in Figure 50. The data from *Experiment 2* (shown in purple), shows the predicted trend and fits well to the shape of the models for radii greater than ~ 10 mm. There is one anomalous data point at $r = -0.06$ m, which may be due to an air pocket being trapped there, hence some small melting may have opened up a hole. The data is not perfectly symmetric, which may be due to the ice surface not being perfectly level and smooth so that the water did not run completely evenly over its surface. This was observed during experiments.

The results of *Experiment 1* do not fit to the models or the data obtained in the second experiment. This is thought to be a result of the freezer lid being open during this experiment so that the experiment could be observed and recorded. The air temperature in the freezer, though less than ambient may have been warmer than in other experiments. Convection to the air from the water whilst it is flowing over the ice surface is known to be negligible. However, the cooling in the pipe may have been reduced leading to a higher than expected water temperature flowing over the ice surface. This would fit with the observed data of significantly more melting across the whole disk. The experiment shows the importance of maintaining the same conditions between experiments and the difficulty in obtaining the desired water temperature without direct measurement.

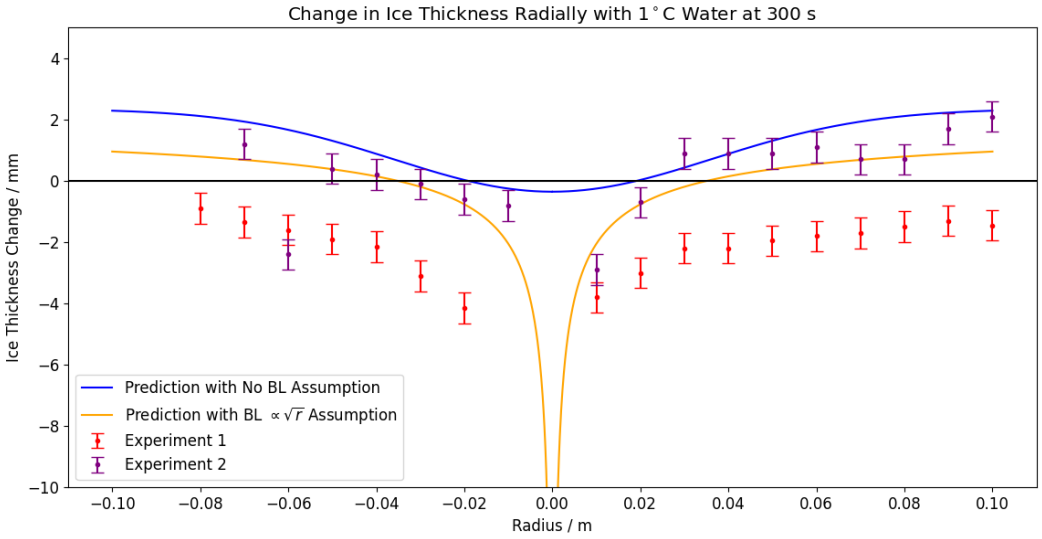

Figure 50: Radial Results for 1.0°C Inlet Water

Neither model captured the observed radial profile in the experiments where the water was injected. Directly underneath the water pipe injecting the water, a circular region of melting was observed with a very steep gradient, outside of this region the ice profile varied as expected. The accuracy and frequency (along the radius) of measurements did not capture the shape of this profile, hence an approximate diagram is shown in Figure 51. The diameter of the hole was the same order of magnitude as the diameter of the supply pipe (9 mm) and approximately 10 – 15 mm deep after five minutes. The models assume that water is injected with a point source at the origin and hence are not representative of the true flow very close to the centre of the ice disk. The water was also impacting on the ice which may have affected the ice profile in the local vicinity. A photo showing the melting seen in the centre of the ice disk is shown in Figure 52.

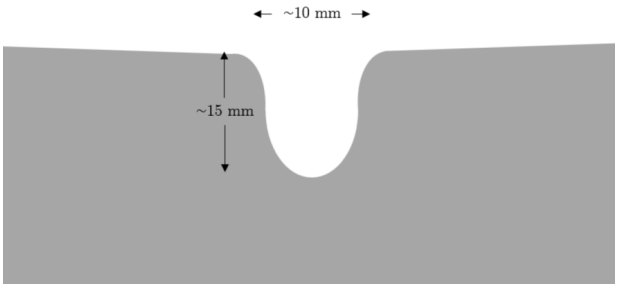

Figure 51: Observed Radial Profile

Figure 52: Melting at the Centre

8.2 Additional Observations - Radial Case

When freezing the initial ice disk a frequent issue was the development of pockets of air underneath the surface of the ice; melting through these to create a solid disk of ice hindered the experiments. These pockets are thought to have formed in the radial case rather than the channel case due to the increased surface area of the ice and smaller area (of walls) for nucleation. Examples of these are shown in Figures 53, 54 and 55.

Figure 53: Air Pockets

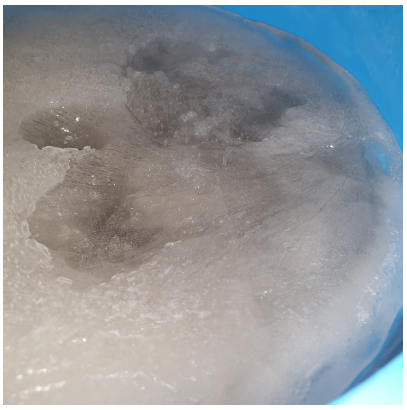

Figure 54: Exposed Pocket(s)

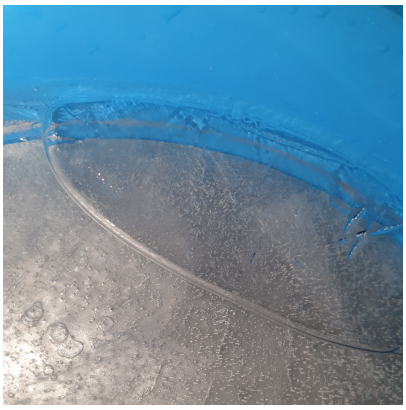

Figure 55: Air Pocket

9 Conclusions

Channel Flow

The initial aim of the project was assess and improve upon the models developed by Cartlidge, 2022 for the development of an ice profile down a channel with water flowing over its surface. A new model was devised considering a thermal boundary layer developing in a shear velocity flow (rather than a uniform one). The experimental setup used previously was supplemented with a Raspberry Pi and thermocouples used to measure the temperature of the water flowing over the ice more accurately. Though this temperature could not be measured directly it was determined through the measurement of the water reservoir temperature.

The results for 0.5°C water flowing down the channel were reliable, showing that the inlet temperature did require careful measurement. The new model with a thermal boundary layer growing in a viscous shear flow accurately predicted the freezing observed after 5 cm down the entire length of the channel with the minimum root mean square error of any of the models. The boundary layer models break down at $x = 0$ and predict infinite melting there for $t > 0$; this is not observed. However, there is significant melting very close to the inlet which reduces very rapidly with distance so the models closely fit to the shape of the observed profile there. The 0.8°C experiment showed very similar behaviour to the 0.5°C case with slightly more melting and slightly less freezing observed. The new thermal boundary layer model again most accurately predicted the ice profile after eight minutes as expected.

The experiments for 2.0°C water were not accurately predicted by the models though the two set of results were reliable. The increased melting of ice further along the channel invalidating the assumptions of the models may explain this. The models all assume that the water flows over the ice as a thin film. With the melting and small inclination angle of the channel the water pools close to the channel inlet and so breaks this assumption. The melting also invalidates the approximation of small changes to the ice-water interface height.

Radial Flow

Developing the models and experiments to a radial flow provides a better representation of the ice volcano than the channel case. Neglecting any velocity boundary layer in the water, the mass flow rate per unit area decreases with $1/r$. For water with no thermal boundary layer the flow temperature (and therefore convective heat transfer) decreases exponentially as $\exp(-r^2)$, significantly faster than for the channel case, hence more freezing is predicted for longer. Assuming a thermal boundary layer growing with $\sqrt{r}$ the heat transfer is identical to the case of the channel with severe melting where the water is injected. The models predict the shape of the data for the region where there is freezing but, as with the channel flow, fail to capture the behaviour of the melting. The discrepancy in the melting region is increased by the approximation of a infinitesimally small source which is not used for experiments. Maintaining constant conditions between experiments was more challenging in the smaller, chest freezer as a result of its smaller volume and hence thermal mass. The second of the two experiments for the radial flow align closely to the predictions, especially in the region of interest where there is freezing. These experiments show that significant further work is required to understand whether ice volcanoes are a feasible way of refreezing the Arctic.

10 Further Research

Behaviour of Salt Water

Saltwater has different properties to the fresh water analysed and used in experiments in this project. For sea water to freeze in the Arctic the top 100-150 metres must cool to -1.8°C. The ice that then forms will not be pure but contains brine (National Snow and Ice Data Center, n.d.). The brine in Arctic ice slowly moves back into the sea by various mechanisms, hence multi-year ice is much stronger and more resistant to melting. The behaviour and implications of this brine when saltwater freezes on the top surface of the ice rather than underneath it must be investigated to determine whether there are any undesirable effects. Modelling the ice profile when using saltwater will be more challenging as the salinity of the ice that forms will not be trivial to determine analytically. The destination of the salt may need to be determined primarily experimental results if it cannot be derived mathematically.

Melting at the Channel Inlet

For ice volcanoes to be successful they need to produce a net increase in the amount (and ideally thickness) of ice. If there is melting where the water is pumped onto the ice then the ice volcano will melt a hole around itself making it useless. The solution to this could be to pump water intermittently, allowing the hole to fill with water that then freezes into a small bump (due to the reduced density of ice) before resuming pumping. The technique may be infeasible as ice volcano may freeze up without a constant flow of water. Also, the overall flow rate must be high enough to produce the required freezing for the ice to survive the summer, intermittent pumping will reduce this.

Cooling the Water to Phase Change Temperature by Convection

Cooling the water to the phase change temperature would prevent it from melting the ice (even if it does not freeze), thereby increasing the effectiveness of the ice volcano. One way this could be prevented is by spraying the water such that it cools to freezing temperature by convection to the air and then freezes by other means. The energy released to cool water per degree Celsius is around 1% of the latent heat of freezing so the cooling provided by the air would be minimal but enough to prevent melting.

Energy of the Latent Heat of Freezing

The above suggestion raises the question of where the latent heat of freezing ends up and the implications that may have. It is envisioned that for the ice volcanoes the heat would primarily be radiated into space with minimal/no effect on the Earth's climate. However, due to the temperature difference of the water and air some heat would be transferred to the air via convection. This will be greater than if the ice surface were exposed as the temperature difference is greater. The increased enthalpy of the air may rise through the atmosphere and then be radiated into space in the ideal case. The destination of the energy released must be investigated to ensure that it does not cause negatively impact the climate.

Impact on Local Communities and Wildlife

The impact on wildlife of using ice volcanoes must be considered: thousands or potentially millions of pumps would be required across the Arctic to counter the severe melting that is currently ongoing. The flow of water over the Arctic surface may hinder polar bears and other animals who live there whilst fish and other marine life rely on the underside of the Arctic ice for a food source and to escape predators (Organisation of the Alfred Wegener Institute, 2021). These will need to be considered when it is decided if to implement ice volcanoes and where. The locations where they could be used will be a balance between where they are most effective at thickening the ice and increasing albedo with where they cause minimal disruption to wildlife. Local communities who live and depend upon the Arctic ice will also need to be consulted on whether they believe ice volcanoes are suitable.

New Ice Behaviour in the Summer

The new ice formed from ice volcanoes will likely be saltier than the ice that would have formed on the underneath of the ice and may also be warmer. First-year ice is saltier than multi-year ice as there has not been time for the brine to work its way out so the difference may be small, however the implications of the ice forming on the surface require attention. The increased saltiness of the new ice will perhaps weaken the ice and make it more likely to break apart/melt, although this is likely to be offset by the increased thickness. The newly formed ice is, however, very unlikely to be identical to naturally formed first-year ice. Hence, there is a need for research into the drawbacks, if there are any, during the summer of generating ice using ice volcanoes.

Arctic Ice Management (Desch et al., 2017)

The work of Desch et al., 2017 suggested that ice volcanoes could be used to thicken ice over the Arctic winter with relative ease (from a heat balance perspective). However, modelling and experiments on the early behaviour of ice volcanoes shows that there is a risk they will render themselves useless by melting the ice around themselves. The balance of heat transfer in the initial stages of the ice volcano may cause them to result in net melting rather than the desired net freezing and so the problem is not as simple as it first appeared. As discussed above, the heat released from freezing may have unknown impacts which were not considered before. Whilst it may appear ice volcanoes can thicken Arctic ice, it is not guaranteed. This report shows that more research is needed to understand the feasibility of ice volcanoes and that a large-scale heat balance is insufficient to predict the behaviour of ice volcanoes.

References

Cartlidge, K. (2022). Ice Thickening - Climate Repair [Unpublished manuscript]. *4th Year Project - Cambridge University Engineering Department*.

Desch, S. J., Smith, N., Groppi, C., Vargas, P., Jackson, R., Kalyaan, A., Nguyen, P., Probst, L., Rubin, M. E., & Singleton, H. e. a. (2017). Arctic Ice Management. *Earth's Future*, *5*(1), 107–127. https://doi.org/10.1002/2016ef000410

Dunne, D. (2022). When will the arctic see its first ice-free summer? https://interactive.carbonbrief.org/when-will-the-arctic-see-its-first-ice-free-summer/

Goddard Institute for Space Studies. (2016). The last three octobers are the warmest on record. *NASA - Climate Change: Vital Signs of the Planet*. Retrieved May 25, 2023, from https://climate.nasa.gov/news/2519/the-last-three-octobers-are-the-warmest-on-record/

Huppert, H. E. (1989). Phase changes following the initiation of a hot turbulent flow over a cold solid surface. *Journal of Fluid Mechanics*, *198*, 293–319. https://doi.org/10.1017/s0022112089000145

IPCC. (2018). Global warming of 1.5 ºc. *IPCC*. https://www.ipcc.ch/sr15/

Labe, Z. (2016). Arctic temperatures. https://sites.uci.edu/zlabe/arctic-temperatures/

Lindsey, R., & Scott, M. (2020). Climate change: Arctic sea ice summer minimum — noaa climate.gov. *www.climate.gov*. https://www.climate.gov/news-features/understanding-climate/climate-change-arctic-sea-ice-summer-minimum

Lister, J. R. (1992). Viscous flows down an inclined plane from point and line sources. *Journal of Fluid Mechanics*, *242*, 631–653. https://doi.org/10.1017/S0022112092002520

Moon, T. A., Overeem, I., Druckenmiller, M., Holland, M., Huntington, H., Kling, G., Lovecraft, A. L., Miller, G., Scambos, T., Schädel, C., Schuur, E. A. G., Trochim, E., Wiese, F., Williams, D., & Wong, G. (2019). The expanding footprint of rapid arctic change. *Earth's Future*, *7*, 212–218. https://doi.org/10.1029/2018ef001088

National Snow and Ice Data Center. (n.d.). Science of sea ice. *National SnowIce Data Center*. Retrieved May 26, 2023, from https://nsidc.org/learn/parts-cryosphere/sea-ice/science-sea-ice

Organisation of the Alfred Wegener Institute. (2021). Life in and underneath sea ice - awi. *www.awi.de*. Retrieved May 26, 2023, from https://www.awi.de/en/focus/sea-ice/life-in-and-underneath-sea-ice.html

Pantling, J. (2022). Ice Thickening - Climate Repair [Unpublished Work]. *UROP - Cambridge University Engineering Department*.

Rantanen, M., Karpechko, A. Y., Lipponen, A., Nordling, K., Hyvärinen, O., Ruosteenoja, K., Vihma, T., & Laaksonen, A. (2022). The arctic has warmed nearly four times faster than the globe since 1979. *Communications Earth & Environment*, *3*(1). https://doi.org/10.1038/s43247-022-00498-3

Schweiger, A., Lindsay, R., Zhang, J., Steele, M., Stern, H., & Kwok, R. (2011). Uncertainty in modeled arctic sea ice volume. *Journal of Geophysical Research*, *116*. https://doi.org/10.1029/2011jc007084

Acknowledgements

The project would not have been possible without the support and his feedback throughout of my supervisor Dr Shaun Fitzgerald, Department of Engineering, University of Cambridge. Without the generosity and assistance provided by Jon Witherley and the kitchen staff of Trinity College, Cambridge I would have been unable to conduct the channel experiments and so am indebted to them for allowing me to use the freezer and for checking on me whilst I was inside it. Dr. Charlotte Gladstone, from the BP Institute, University of Cambridge lent me the pump that was used for all the experiments. I am indebted to Professor Hugh Hunt, Department of Engineering, University of Cambridge for his support along with John Aldridge in setting up the Raspberry Pi with the thermocouples despite the many challenges. Gary Bailey, Department of Engineering, University of Cambridge also provided assistance soldering and waterproofing the second set of thermocouples. I am thankful to Professor Grae Worster, Department of Applied Mathematics and Theoretical Physics, University of Cambridge for his guidance when developing the new thermal boundary layer model for channel flow and the models for radial flow. Finally, I would like to thank Stefan Savage, Department of Engineering, University of Cambridge for setting up the new lab with the chest freezer and for building the experimental setup used in the radial experiments.

Retrospective Risk Assessment

The risk assessment submitted at the beginning of the project for working in the walk-in freezer identified the hazards and how these could be avoided. The main risk was hypothermia from being stuck in the freezer at -18°C; this was mitigated by leaving the freezer at regular intervals and being checked on by the kitchen staff at 15 minute intervals whilst working in the kitchens. Throughout the experiments in the kitchens no incidents occurred as a result of the precautions taken.

A second risk assessment was submitted when experiments moved to the chest freezer in the Seawater Lab at the Department of Engineering, University of Cambridge. As the experiments were being conducted from outside the freezer the risk of hypothermia was reduced and the overall was risk lower. There were no incidents while working in the lab.

The risk assessment successfully identified the hazards present when conducting the experiments and the mitigations put in place were suitable to manage these.